Evolutionary conservation and adaptability of neuropeptide function: insights from sulfakinin/cholecystokinin-type signaling in an echinoderm, the sea cucumber Apostichopus japonicus

Huachen Liu
Ocean University of China
Hongliang Yang
Ocean University of China
Xiang Tian
Ocean University of China
Maurice Elphick
Queen Mary University of London
Chen Muyan
chenmuyan@ouc.edu.cn

Ocean University of China

Research Article

Keywords: Sulfakinin/cholecystokinin, Feeding inhibition, Intestinal contraction, Evolutionary adaptability, Echinoderm

Posted Date: March 23rd, 2026

DOI: https://doi.org/10.21203/rs.3.rs-9103845/v1

Additional Declarations: No competing interests reported.

Evolutionary conservation and adaptability of neuropeptide function: insights from sulfakinin/cholecystokinin-type signaling in an echinoderm, the sea cucumber *Apostichopus japonicus*

Huachen Liu [1], Hongliang Yang [1], Xiang Tian [1], Maurice R. Elphick [2] and Muyan Chen [1,*]

1 The Key Laboratory of Mariculture, Ministry of Education, Ocean University of China, Qingdao, China

2 Centre for Evolutionary & Functional Genomics, School of Biological & Behavioural Sciences, Queen Mary University of London, London, United Kingdom

* Correspondence: chenmuyan@ouc.edu.cn;

Abstract

Background: Food ingestion is fundamental for animal survival and growth, with the cessation of feeding upon nutrient fulfillment being tightly regulated by a variety of satiety factors. Notably, sulfakinin/cholecystokinin (SK/CCK)-type neuropeptide signaling has been identified as an inhibitory regulator of food intake across the animal kingdom. However, its regulatory mechanism in feeding in deuterostome invertebrates remains unclear. Here, we characterized SK/CCK-type signaling in a deuterostome invertebrate, the sea cucumber *Apostichopus japonicus* (phylum Echinodermata).

Results: A single SK/CCK-type precursor in *A. japonicus* generates two mature peptides (AjSK/CCK1, AjSK/CCK2) that activate a shared receptor (AjSK/CCKR), triggering Ca^{2+} mobilization via the Gαq-dependent pathway and extracellular signal regulated kinase 1/2 (ERK1/2) phosphorylation. Both peptides induce dose-dependent contraction of longitudinal muscles, while AjSK/CCK2 additionally elicits sustained contraction of the posterior intestine, an effect absent in other gut regions. Long-term injection of both peptides reduces food intake and significantly downregulates orexin-type neuropeptide genes (*AjOrexin1P*, *AjOrexin2P*) in the circumoral nerve ring (CNR) and intestine.

Conclusion: Unlike mammals, where CCK inhibits feeding by contracting the pyloric sphincter to delay gastric emptying, SK/CCK-type peptides in sea cucumbers exert their anorexic effect

in part by selectively contracting the posterior intestine, thereby inhibiting intestinal emptying. This divergence in action sites highlights the evolutionary adaptability of SK/CCK-type signaling as a conserved inhibitory regulator of feeding across bilaterian animals. Elucidating these mechanisms in the economically important *A. japonicus* may inform development of appetite-promoting agents for sustainable aquaculture.

Graphical abstract

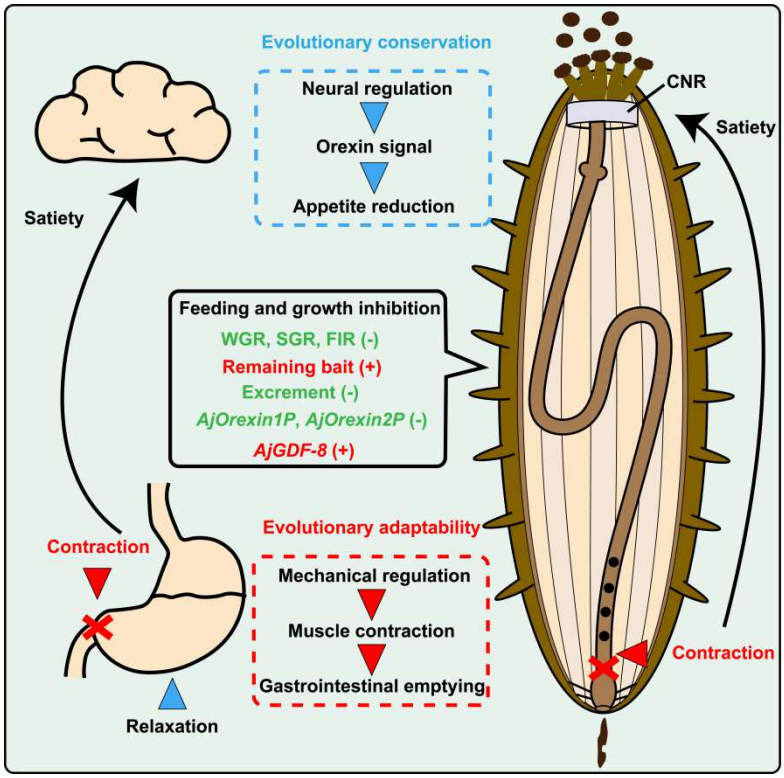

The feeding inhibition mechanism of SK/CCK-type neuropeptides: sea cucumber vs. mammal

In mammals and sea cucumbers, SK/CCK-type neuropeptides inhibit feeding via a dual-pathway mechanism: 1) Neural regulation: downregulating expression of the orexigenic factor Orexin in the central nervous system to reduce appetite, and the conserved interaction between SK/CCK and Orexin in feeding regulation, from deuterostome invertebrates to mammals, highlights the evolutionary conservation of neuropeptide function; 2) Mechanical regulation: contracting the pyloric sphincter (mammals) or posterior intestine (sea cucumbers) to inhibit gastric or intestinal emptying, and this divergence in action sites reflects the evolutionary adaptability of neuropeptide function.

Keywords: Sulfakinin/cholecystokinin, Feeding inhibition, Intestinal contraction, Evolutionary adaptability, Echinoderm

Background

Feeding is a fundamental physiological process essential for the survival, growth, and energy homeostasis of animals, and this complex behavior is regulated by the integration of diverse external environmental cues and internal physiological states. When an animal's nutritional and energy requirements are satisfied, a series of satiety signals are elicited to suppress further food intake (1-4). Digestion and nutrient processing occur primarily in the gastrointestinal tract, while the state of satiety is integrated within the central nervous system. Accordingly, certain satiety factors act peripherally by modulating gastrointestinal motility to mechanically limit food intake, whereas others function centrally by directly suppressing appetite through interactions with neural circuits (5-9). These complementary mechanisms illustrate that the regulation of feeding involves coordinated interactions between neurological and gastrointestinal systems, with neuropeptides serving as key mediators of this coordination.

As evolutionarily conserved signaling molecules, neuropeptides represent the largest and most diverse class of neuromodulators, mediating communication between the brain and peripheral tissues to regulate physiological processes and behaviors across the animal kingdom, including satiety. Numerous neuropeptides have been identified as satiety factors, including sulfakinin/cholecystokinin (SK/CCK)-type, vasopressin/oxytocin (VP/OT)-type, kisspeptin (Kiss)-type and glucagon-like peptide-1 (GLP-1), which suppress feeding through distinct mechanisms (10-16).

The peptide hormone CCK was first discovered in 1928 and was named on account of its effect in causing gallbladder contraction (17). An inhibitory effect of CCK on feeding was first reported in 1972, with intraperitoneal injection of CCK significantly reducing food intake and water consumption in mice (18). Since then, a growing number of studies have investigated the role of CCK in vertebrates, not only in inhibiting feeding, but also in other physiological processes, including learning, memory, anxiogenesis and inflammation (19, 20). In mammals, CCK has the same C-terminal structure (Trp-Met-Asp-Phe-NH_2) as gastrin, a related peptide

hormone derived from a different precursor protein, which reflects a common evolutionary origin (21, 22). Phylogenetic analysis indicates that the common ancestor of vertebrates acquired genes encoding CCK and gastrin through genome duplication events, whereas only one gene encoding a CCK/gastrin-like peptide occurs in invertebrate chordates (e.g. cionin in the urochordate *Ciona intestinalis*) (23, 24). In non-chordates, a myotropic neuropeptide isolated from the cockroach *Leucophaea maderae*, and named leucosulfakinin, shares sequence similarity with vertebrate CCK/gastrin-type peptides (25). Subsequent studies have identified numerous sulfakinin (SK)/CCK-type neuropeptides in invertebrates, including molluscs, annelids, nematodes and echinoderms, supporting the hypothesis that SK/CCK-type signaling originated in a common ancestor of the Bilateria (13, 26-28). Conserved features of SK/CCK-type peptides are an amidated aromatic amino-acid (typically phenylalanine) at the C-terminus and a sulphated tyrosine at a position 6-8 residues before the C-terminus, and both of these post-translational modifications are typically critical for the bioactivity of the mature peptides (8, 13, 28).

In vertebrates, CCK exerts its effects by binding to two G-protein-coupled receptors: CCKR1 and CCKR2, and CCKR1 is selectively activated by sulphated CCK, while CCKR2 binds both sulphated and non-sulphated forms of CCK and gastrin (29-32). The inhibitory effects of CCK on feeding mediated by these receptors have been studied extensively in mammals. Neurologically, when mammals ingest food and experience gastric distension, CCK is released from enteroendocrine cells and activates adjacent vagal afferent neurons, propagating signals to the brainstem. Post-ingestive feedback from the brainstem is then transmitted to the gastrointestinal tract, leading to reduced food intake (5, 6, 8). Mechanistically, CCK regulates gastrointestinal peristalsis by affecting smooth muscle activity in regions of the gut, causing contraction of the pyloric sphincter and relaxation of the stomach fundus, thereby inhibiting gastric emptying and further reducing food intake (7, 19, 33, 34). GPCRs homologous to vertebrate CCK receptors have been identified and pharmacologically characterized in many invertebrates, although the number of receptors varies among species. For instance, two SKRs are present in *Drosophila melanogaster* and two CCK-type peptide receptors (CKR1 and CKR2) exist in *Caenorhabditis elegans*, with CKR2 having two splice isoforms (35, 36). Only one SK/CCK-type receptor has been identified in the starfish *Asterias rubens* (phylum

Echinodermata), whilst the SK signaling system has been lost in some insects (13, 26, 37). Despite these variations, the SK/CCK signaling systems in invertebrates share functional similarities with vertebrates, including roles in inhibition of feeding, regulation of intestinal motility and modulation of digestive enzyme secretion (4, 13, 28, 38). These findings collectively indicate that SK/CCK-type neuropeptides retain an ancient and evolutionarily conserved role in inhibitory regulation of feeding across bilaterian animals.

The sea cucumber *A. japonicus* (phylum Echinodermata), is a commercially important aquaculture species in Asia, prized for its significant nutritional and medicinal value (39, 40). However, with the continuous expansion of market demand, significant challenges have emerged in *A. japonicus* aquaculture. As feeding behavior directly correlates with aquaculture yield, elucidating the molecular mechanisms regulating feeding in this species may provide critical insights for improving aquaculture efficiency. In the present study, we identified and characterized the SK/CCK signaling system in *A. japonicus*, including characterization of a SK/CCK-type receptor, analysis of the expression profile of the SK/CCK-type precursor and receptor and investigation of the *in vitro* and *in vivo* pharmacological effects of SK/CCK-type peptides in this species. Furthermore, we analyzed the mechanisms by which SK/CCK-type neuropeptides act as satiety factors to mediate inhibition of feeding and growth in sea cucumber.

Results

Molecular characterization of the SK/CCK-type precursor in *A. japonicus*

A full-length cDNA with a 492 bp ORF encoding the 163-amino acid SK/CCK-type precursor (AjSK/CCKP) protein was identified in *A. japonicus*. Structural characterization reveals that this precursor comprises: 1) an N-terminal signal peptide, 2) two predicted SK/CCK-type neuropeptides (AjSK/CCK1 and AjSK/CCK2), 3) four proteolytic cleavage sites (R/KR motifs), and 4) glycine residues located before the C-terminal cleavage sites, which are necessary for amidation **(Fig. 1A; Additional file 1: Fig. S1A)**. Gene structure analysis revealed that SK/CCK-type precursors across the Echinodermata are encoded by a single exon **(Fig. 1B)**. However, interspecific variation exists in the number of SK/CCK-type neuropeptides derived

from these precursors: in echinoids and ophiuroids there are three, in holothuroids and asteroids there are two, and in crinoids there is one **(Additional file 1: Fig. S1B)**. The predicted three-dimensional structure of the AjSK/CCKP protein is shown in **Fig. 1C**, with a predicted molecular mass of 18.21 kDa.

Multiple sequence alignment of SK/CCK-type neuropeptides from *A. japonicus* with those from other taxa reveals a conserved tyrosine residue, a pan-bilaterian characteristic of this neuropeptide family. The tyrosine residue is typically sulphated and this post-translational modification is often critical for bioactivity **(Fig. 1D)**. Notably, mass spectrometric analyses of *A. rubens* radial nerve cord extracts have identified non-sulphated variants of SK/CCK-type neuropeptides, but these demonstrate only weakly detectable physiological activity (13). Among holothurians (*A. japonicus*, *Stichopus horrens*, and *Holothuria leucospilota*), the SK/CCK-type neuropeptides display remarkable sequence conservation, characterized by a core Asp-Tyr-(Gly/Asn)-Asp-Leu-Gly-(Met/Phe)-Phe-Phe (DYG/NDLGM/FFF) motif **(Fig. 1D)**, indicative of strong evolutionary constraints on functional domains. Using the CLANS method based on BLASTp e-values for sequence similarity clustering, we analyzed echinoderm SK/CCK-type precursors. They formed a compact subgroup most closely related to a hemichordate precursor, while also showing positive BLAST matches with those from other taxonomic groups **(Fig. 1E)**.

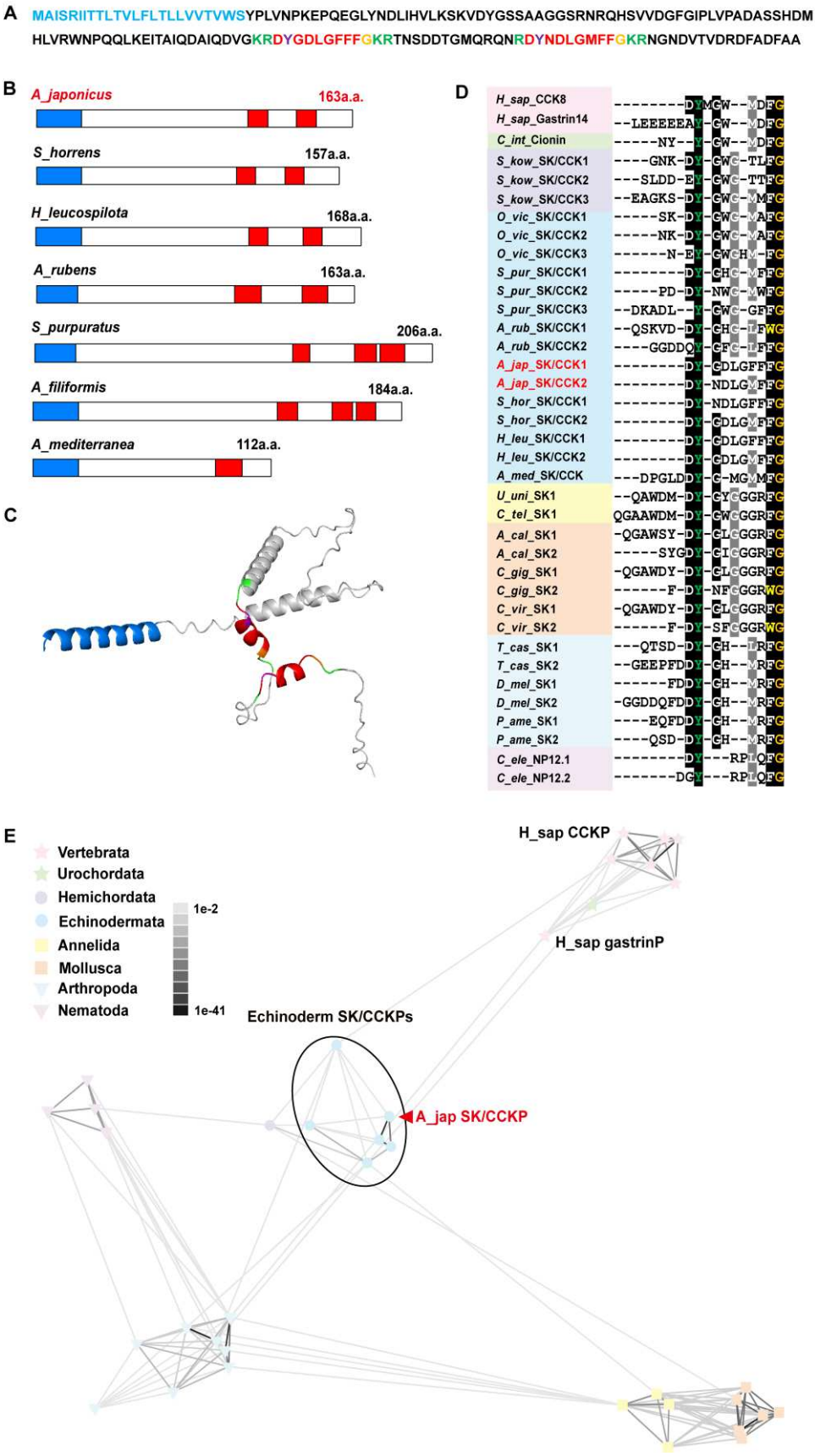

Figure 1. Characterization of the SK/CCK-type precursor in *A. japonicus*

A. Amino acid sequence of AjSK/CCKP. The predicted signal peptide is highlighted in blue,

potential proteolytic cleavage sites in green, and SK/CCK-type peptides in red. C-terminal glycine (G) residues, putative substrates for amidation, are shown in orange and tyrosine (Y) residues predicted to be sulphated are in purple. **B**. Comparison of the structure of SK/CCK-type neuropeptide precursors across Echinodermata. Blue boxes indicate signal peptides, red boxes represent SK/CCK-type peptides and white boxes represent other regions of the precursor proteins. **C**. The predicted tertiary structure of AjSK/CCKP visualised using SWISS-MODEL and with different regions colored as in panel A. **D.** Sequence alignment of AjSK/CCK1 and AjSK/CCK2 with SK/CCK-type peptides from other taxa. Tyrosine (Y) residues (potential sulphation sites) are in green, C-terminal tryptophan (W) residues (an atypical feature) are in yellow, and C-terminal glycine (G) residues (putative amidation substrates) are in orange. Species belonging to different taxa are highlighted with different colors: pink (Vertebrata), green (Urochordata), purple (Hemichordata), blue (Echinodermata), yellow (Annelida), orange (Mollusca), light blue (Arthropoda) and light purple (Nematoda). **E**. A BLOSUM62 cluster map depicting sequence similarity between echinoderm SK/CCK-type precursors and those from other taxa. Nodes are colored by phylum (see key). Connections represent BLAST relationships ($P \leq$1e-2). SK/CCK-type precursors from echinoderms are highlighted with a black circle, and the AjSKCCKP precursor is labeled in red. Species abbreviations and accession numbers of the sequences used in multiple sequence alignment and clustering analysis are listed in **Additional file 2: Dataset S1**.

Identification of an SK/CCK-type receptor in *A. japonicus*

Using the pharmacologically characterized SK/CCK receptor from *A. rubens* as a query, a bioinformatic analysis of the *A. japonicus* CNR transcriptome via BLAST homology screening identified a single candidate SK/CCK-type receptor transcript, which contains a 1,317 bp ORF encoding a 439-amino acid receptor protein harboring 43 putative phosphorylation sites **(Additional file 1: Fig. S2A)**. Phylogenetic analysis robustly supported the identification of this protein as a SK/CCK-type receptor and therefore hitherto it is referred to as *A. japonicus* SK/CCK-type receptor (AjSK/CCKR). AjSK/CCKR is positioned in a branch of the tree together with other echinoderm SK/CCK-type receptors, which is then grouped with the hemichordate *S. kowalevskii* ortholog to form an ambulacrarian clade. This entire ambulacrarian group is

nested within a broader deuterostome clade that includes chordate CCK receptors, encompassing pharmacologically characterized CCK1R and CCK2R from human, mouse and *Gallus gallus*, as well as the cionin receptors CioR1 and CioR2 from *C. intestinalis*. Finally, this deuterostome clade is grouped with protostome SK/CCK receptors to form a single bilaterian SK/CCK receptor clade **(Fig. 2)**.

Structural characterization revealed that AjSK/CCKR contains seven transmembrane domains joined by extracellular and cytoplasmic loops, a hallmark feature of GPCRs, and a potential N-glycosylation site was identified within the extracellular N-terminal region **(Additional file 1: Fig. S2B)**. Furthermore, a large intracellular linker between transmembrane domain V and VI was observed, which is a noticeable feature previously reported for insect SK/CCK receptors (37). The tertiary structure of AjSK/CCKR was predicted and is shown in **Additional file 1: Fig. S2C**, with a predicted molecular mass of 49.44 kDa.

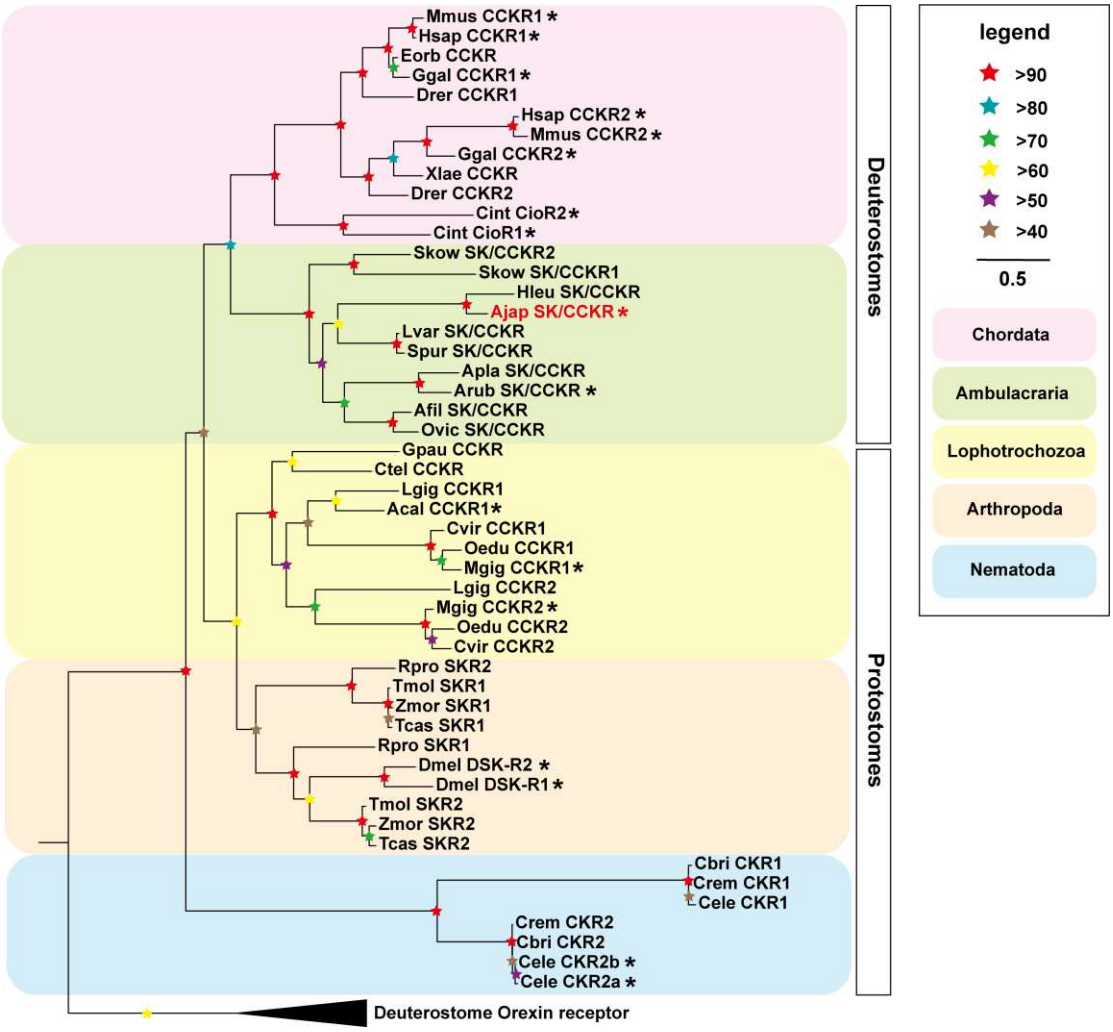

Figure 2. Maximum-likelihood phylogenetic tree of bilaterian SK/CCK-type receptors

The tree was constructed using the IQ-tree server, with bootstrap support (1000 replicates) indicated at nodes. Deuterostome orexin-type receptors were used as the outgroup and branch lengths are proportional to evolutionary distance. The asterisk (*) denotes receptors that have been pharmacologically characterized with identified SK/CCK ligands. Species abbreviations and accession numbers of the sequences used in phylogenetic analysis are listed in **Additional file 3: Dataset S2**.

AjSK/CCK1 and AjSK/CCK2 act as ligands to activate AjSK/CCKR

A HEK293T-AjSK/CCKR-G5A cell system was used to test AjSK/CCK1, AjSK/CCK2, AjSK/CCK1ns and AjSK/CCK2ns as candidate ligands for AjSK/CCKR at concentrations ranging from 10^{-4} M to 10^{-14} M. The results showed that the sulphated peptides AjSK/CCK1 and AjSK/CCK2 induced a dose-dependent bioluminescence signal with comparable potency, and the values of half-maximal response concentrations (EC_{50}) were 2.06×10^{-9} M and 3.92×10^{-9} M, respectively **(Fig. 3A)**. However, when comparing the maximal responses elicited by the two peptides, AjSK/CCK2 exhibited significantly higher activation efficacy than AjSK/CCK1 at the highest concentration tested (10^{-4} M) **(Fig. 3B)**. The non-sulphated variants AjSK/CCK1ns and AjSK/CCK2ns elicited only weak signals, with EC_{50} values of 2.33×10^{-6} M and 7.72×10^{-6} M **(Fig. 3A)**, and maximal efficacies of 31.52% and 38.84%, respectively, relative to their sulphated counterparts, indicating that tyrosine sulphation is essential for effective receptor activation of SK/CCK-type neuropeptides in *A. japonicus*. No response was observed in empty vector-transfected controls.

Subsequently, to further analyze the downstream signaling pathways of AjSK/CCKR, we employed SRE-Luc and CRE-Luc reporter systems to assess PKC and PKA activation, respectively (41). The results showed that both AjSK/CCK1 and AjSK/CCK2 increased SRE luciferase activity in a concentration-dependent manner at concentrations ranging from 1×10^{-4} M to 1×10^{-14} M in HEK293 cells expressing AjSK/CCKR, with EC_{50} values of 2.66×10^{-9} M and 4.65×10^{-9} M, respectively **(Fig. 3C)**. No activity was observed in empty vector-transfected controls. However, when using the CRE-Leu reporter system, neither AjSK/CCK1 nor AjSK/CCK2 caused changes in luciferase activity, even at concentrations as high as 10^{-5} M (data not shown). It has been reported that CCK causes ERK1/2 phosphorylation to mediate

feeding inhibition in rat, and therefore we investigated whether AjSK/CCK1 and AjSK/CCK2 can cause the activation of the ERK1/2 signaling cascade (42). The results showed that AjSK/CCK1 and AjSK/CCK2 cause significantly increased ERK1/2 phosphorylation at 30min and 15min compared with 0min, followed by dephosphorylation at 45min and 30min, respectively **(Fig. 3D)**. These results indicate that AjSK/CCK1 and AjSK/CCK2 are functional ligands for AjSK/CCKR, which activate the Gαq/Ca^{2+}/PKC signaling pathway and induce downstream ERK1/2 phosphorylation, but do not activate the cAMP/PKA signaling pathway.

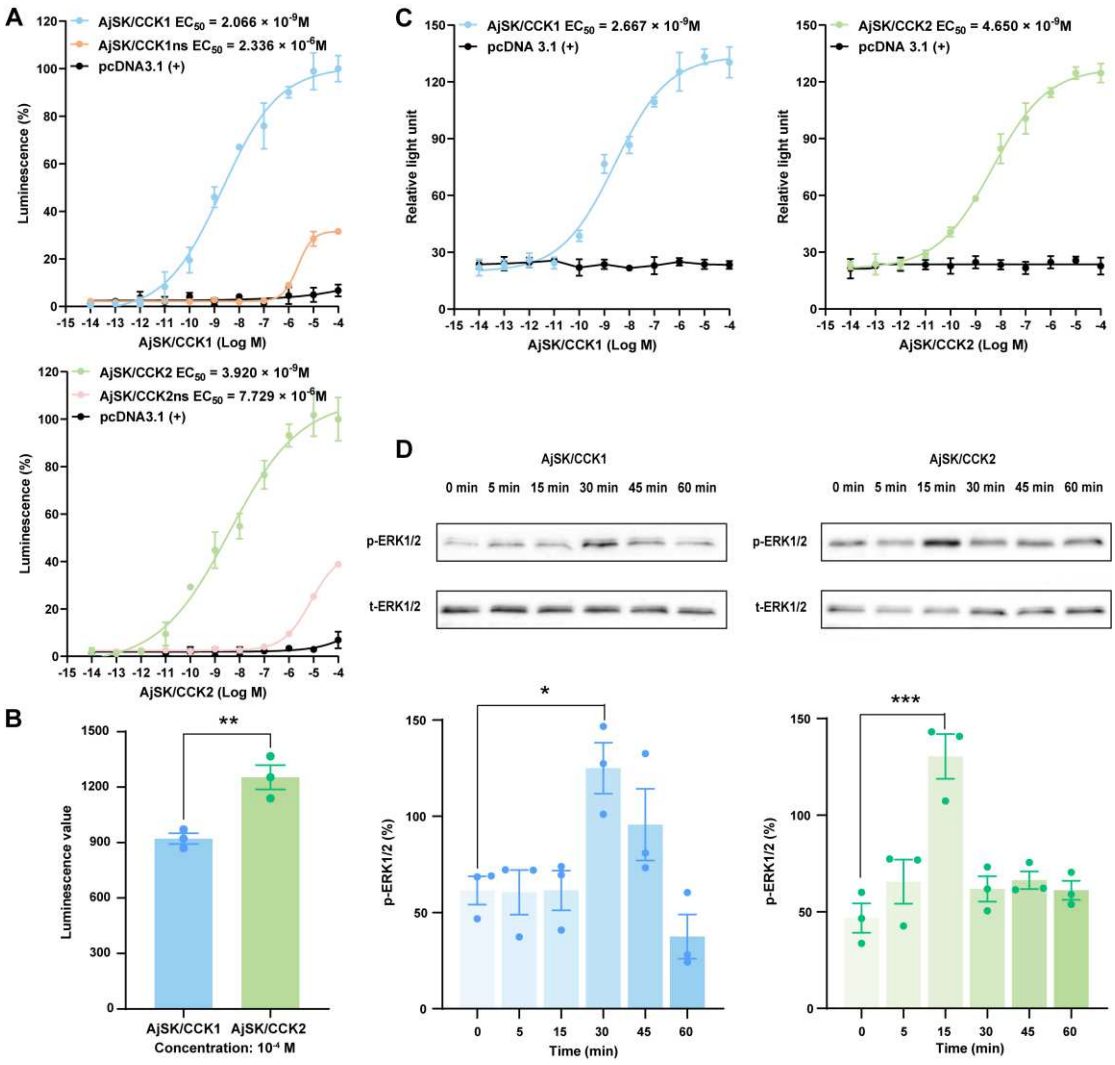

Figure 3. Functional characteristics of the AjSK/CCK signaling system

A. The sulphated peptides AjSK/CCK1, AjSK/CCK2 and the non-sulphated peptides AjSK/CCK1ns, AjSK/CCK2ns, trigger dose-dependent luminescence in HEK293T cells expressing AjSK/CCKR and G5A. Luminescence values were normalized to the maximal response in each experiment (n=3). **B**. The luminescence values caused by the activation of AjSK/CCKR by AjSK/CCK1 and AjSK/CCK2 at a concentration of 10^{-4}M (n=3). **C**. Induction of

SRE-driven luciferase activity by AjSK/CCK1 and AjSK/CCK2 in HEK293T cells expressing AjSK/CCKR (n=3). **D**. Immunoblot intensity of representative bands and the expression levels of p-ERK1/2, normalized based on t-ERK1/2, after treatment with AjSK/CCK1 ($F_{(5, 12)}$=6.189) or AjSK/CCK2 ($F_{(5, 12)}$=12.67) for indicated times (n=3). Asterisks represent the significant difference as follows: *: $p \leq 0.05$, **: $p \leq 0.01$, ***: $p \leq 0.001$.

Molecular simulation of the interaction between AjSK/CCK1, AjSK/CCK2 with AjSK/CCKR

AjSK/CCK1 and AjSK/CCK2 differ at two amino acid residues, specifically at positions 3 (AjSK/CCK1: Gly, AjSK/CCK2: Asn) and 7 (AjSK/CCK1: Phe, AjSK/CCK2: Met) and they exhibit significantly different maximal efficacy in receptor activation **(Fig. 3B)**. To further explore the structural basis for this functional divergence, we investigated potential differences in their interaction sites with the receptor, with homology modeling performed using AlphaFold3 and molecular docking carried out with AutoDock Vina. The results showed the calculated binding energies for AjSK/CCK1 and AjSK/CCK2 with AjSK/CCKR were −9.7 kcal/mol and −9.3 kcal/mol, respectively **(Fig. 4)**. Based on the defined thresholds where a binding energy of ≤ −5 kcal/mol indicates effective binding and ≤ −7 kcal/mol represents strong binding, both ligands demonstrate comparable high-affinity interactions, which provide reliable references for further analysis (43). Subsequently, the docking models were imported into PyMOL and LigPlot+ to analyze the key amino acid residues involved in ligand-receptor interactions.

Detailed pose analysis indicates that both AjSK/CCK1 and AjSK/CCK2 anchor within the binding pocket of AjSK/CCKR primarily through hydrogen bonds, salt bridges, and hydrophobic interactions. In the case of AjSK/CCK1, residues Asp1, Gly3, Asp4, and Leu5 are predicted to form hydrogen bonds with Asn341, Arg203, Lys201, and Arg366 of AjSK/CCKR, with bond lengths of 2.97 Å, 3.05 Å, 2.96 Å, and 2.8 Å, respectively. In addition, Asp1 and Asp4 are predicted to collectively form four salt bridges with Arg366 and Lys201 **(Fig. 4A)**. For AjSK/CCK2, Tyr2, Asn3, Asp4, and Met7 are predicted to participate in the formation of seven hydrogen bonds with Arg203, Arg366, Lys201, and His204 of AjSK/CCKR, and the corresponding bond lengths are 2.8 Å, 3.05 Å, 3.16 Å, 2.9 Å, 3.14 Å, 2.79 Å, and 2.83 Å. Asp1 and Asp4 in AjSK/CCK2 are predicted to contribute four salt bridges to interactions with Arg356

and Lys201 in AjSK/CCKR **(Fig. 4B)**. Compared to AjSK/CCK2, AjSK/CCK1 is predicted to form fewer hydrogen bonds with the receptor and have a lower binding energy. Comparative analysis of the divergent residues revealed distinct interaction patterns: in AjSK/CCK2, both Asn3 and Met7 are predicted to participate in hydrogen bonding, whereas in AjSK/CCK1, only Gly3 is predicted to form such interactions. However, the presence of Phe7 in AjSK/CCK1 contributes to a continuous triple-phenylalanine motif at its C-terminus. This hydrophobic cluster is predicted to engage with the receptor binding pocket via extensive hydrophobic contacts mediated by the benzene rings **(Fig. 4A, the part marked by the red circle)**. In conclusion, AjSK/CCK1 binding is predicted to rely more substantially on hydrophobic interactions, while AjSK/CCK2 bimding is predicted to depend more heavily on hydrogen bonding.

We performed sequence alignment between AjSK/CCKR and human CCKR1 to identify the conserved key residues known or predicted to be involved in ligand binding. Nobtably, use of cryo-electron microscopy has resolved the structure of human CCKR1 in complex with its natural ligand (CCK-8), revealing a structural basis for its stronger affinity for the sulphated peptide than the non-sulphated peptide (44, 45). Our analysis revealed eight conserved residues in both AjSK/CCKR and human CCKR1 that are predicted or known, respectievly, to participate in ligand binding. Notably, Arg203 and Asn341 in AjSK/CCKR and the corresponding residues Arg197 and Asn333 in human CCKR1, are predicted or known to form hydrogen bonds with their respective ligands (44, 46) **(Additional file 1: Fig. S3)**.

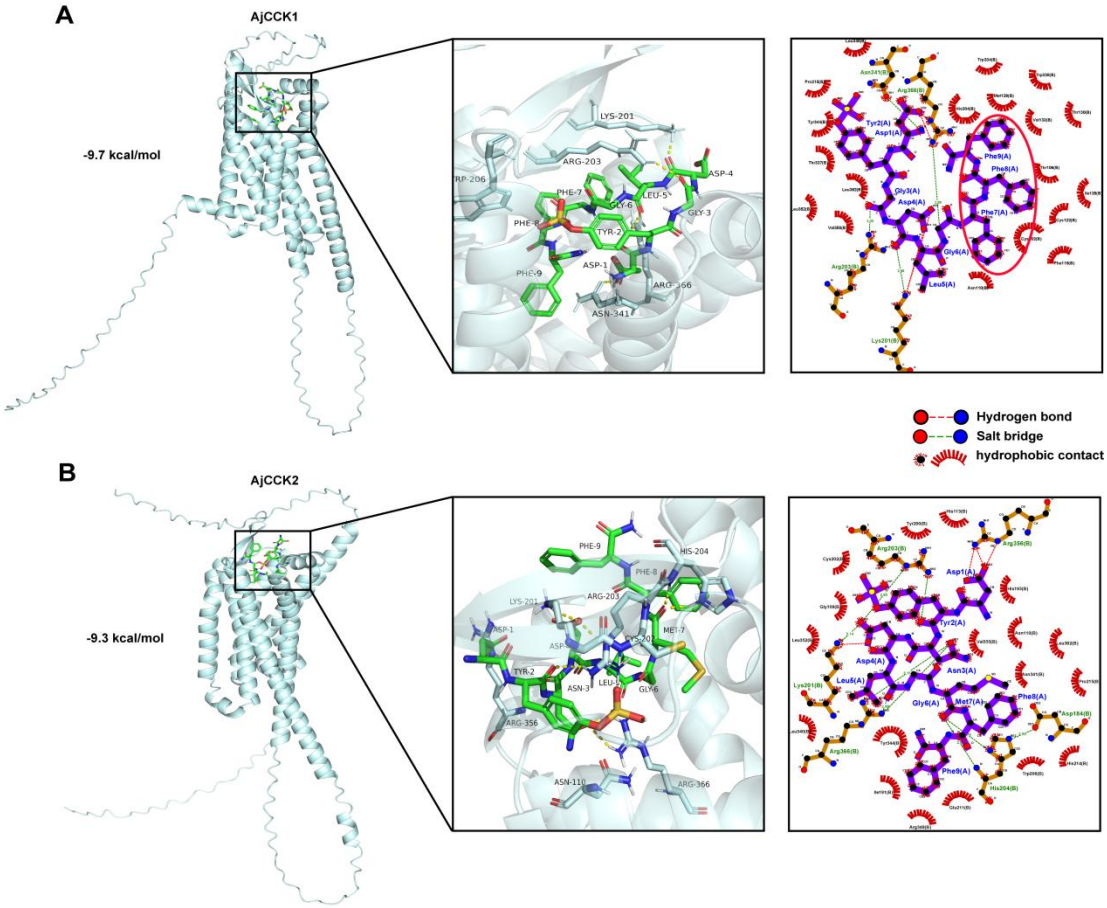

299

300 **Figure 4. Molecular docking of AjSK/CCKs-AjSK/CCR complex.**

301 **A**. AjSK/CCK1-AjSK/CCR complex. **B**. AjSK/CCK2-AjSK/CCKR complex. Left panels: Overall
302 binding poses of AjSK/CCK1 and AjSK/CCK2 within the receptor binding pocket. The receptor
303 is shown as a blue cartoon; ligands are shown as sticks (C: green, N: blue, O: red, S: yellow).
304 Key interaction regions are boxed. Middle panels: enlarged 3D view of key interaction regions
305 and hydrogen bonds are indicated by yellow dashed lines. Right panels: 2D interaction
306 diagrams, where hydrogen bonds are shown as green dashed lines and labelled with distances
307 (Å), salt bridges are shown as red dashed lines and hydrophobic contacts are represented by
308 jagged arcs. The red circle in A represents the continuous triple-phenylalanine motif in
309 AjSK/CCK1, which is predicted to form extensive hydrophobic contacts with the receptor.

310

311

312 **Expression profile of *AjSK/CCKP* and *AjSK/CCKR* in *A. japonicus***

313 RT-qPCR analysis revealed similar expression profiles for both *AjSK/CCKP* and its
314 receptor *AjSK/CCKR*. The expression of *AjSK/CCKP* was significantly higher in intestinal tissue

than in longitudinal muscle, CNR, respiratory tree, and gonadal tissues **(Fig. 5A)**. Similarly, *AjSK/CCKR* expression was also most abundant in the intestine, with transcript levels significantly higher than those in longitudinal muscle, CNR, respiratory tree, and gonad **(Fig. 5B)**.

AjSK/CCK1 and AjSK/CCK2 cause dose-dependent contraction of *in vitro* muscle preparations from *A. japonicus*

Based on the tissue-specific expression profiles of *AjSK/CCKP* and *AjSK/CCKR* in the longitudinal muscle and intestinal tissues of *A. japonicus*, we prepared longitudinal muscle, esophagus, anterior and posterior intestine preparations to investigate the pharmacological effects of sulphated peptides (AjSK/CCK1, AjSK/CCK2) and non-sulphated variants (AjSK/CCK1ns, AjSK/CCK2ns) *in vitro* **(Additional file 1: Fig. S4)**. We found that both AjSK/CCK1 and AjSK/CCK2 caused dose-dependent contraction of the longitudinal muscle preparations *in vitro* at concentrations between 10^{-8} and 10^{-6} M, with the maximum contraction at 10^{-6} M, but AjSK/CCK2 induced significantly stronger contractions than AjSK/CCK1 **(Fig. 5C)**. AjSK/CCK2 also induced dose-dependent contraction of posterior intestine preparations at concentrations between 10^{-7} and 10^{-5} M. The maximum response was observed at 10^{-5} M, and the induced contraction was characterized as sustained, lasting approximately 60min at this concentration **(Fig. 5D; Additional file 1: Fig. S5)**. Notably, AjSK/CCK2 did not produce any detectable contractile or relaxant effects on esophagus and anterior intestine preparations (data not shown). AjSK/CCK1 had no effect on esophagus, anterior or posterior intestine preparations, and the non-sulphated peptides AjSK/CCK1ns, AjSK/CCK2ns and negative control (PBS with 1% DMSO) showed no activity in any of the preparations tested (data not shown).

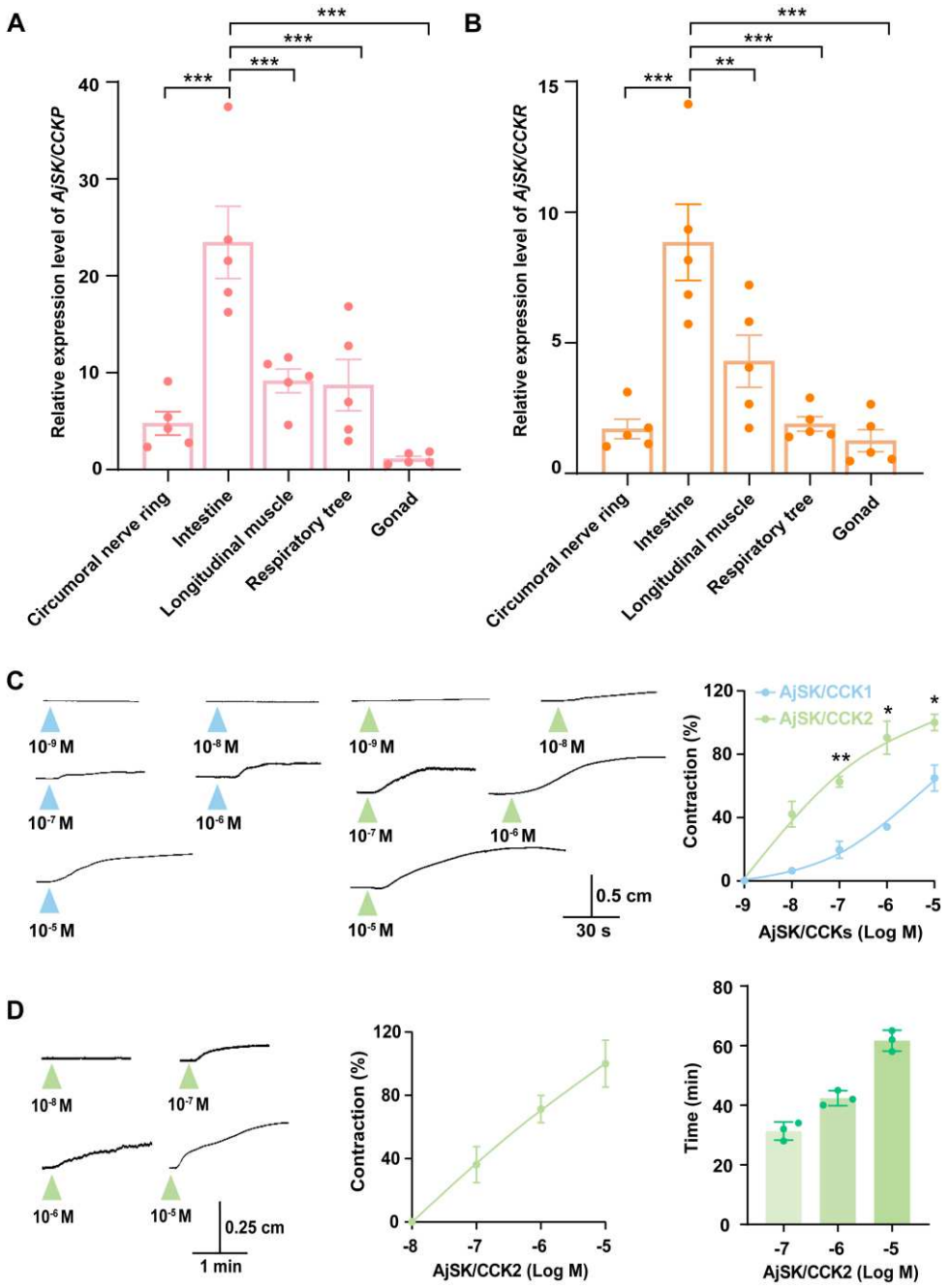

Figure 5. The expression profiles of *AjSK/CCKP* and *AjSK/CCKR* and the pharmacological effects of AjSK/CCKs.

A. The expression profiles of *AjSK/CCKP* ($F_{(4, 20)}$=15.07). **B**. The expression profiles of *AjSK/CCKR* ($F_{(4, 20)}$=14.20). The relative expression level of each tissue was compared with that of the gonad, and the intestine was selected as the control group for significance analysis (n=5). **C**. Representative recordings showing that AjSK/CCK1 and AjSK/CCK2 cause contraction of longitudinal muscle preparations and concentration-response curve for AjSK/CCK1 and AjSK/CCK2 induced contraction at concentrations between 10^{-9} and 10^{-6} M

(n=3). And AjSK/CCK2 induced significantly greater contraction than AjSK/CCK1 at 10^{-8} M, 10^{-7} M, 10^{-6} M and 10^{-5} M (treatment: $F_{(1, 4)}$=306.2).The responses are expressed as the mean percentage of longitudinal muscle contraction induced by 10^{-6} M AjSK/CCK2. **D**. Representative recordings showing that AjSK/CCK2 causes contraction of posterior intestine preparations, concentration-response curve for AjSK/CCK2 induced contraction at concentrations between 10^{-8} and 10^{-5} M, and duration of intestinal contraction induced by AjSK/CCK2 (n=3). The responses are expressed as the mean percentage of posterior intestine contraction induced by 10^{-5} M AjSK/CCK2. Asterisks represent significant differences as follows: **: $p \leq 0.01$, ***: $p \leq 0.001$.

AjSK/CCK1 and AjSK/CCK2 inhibit feeding and growth in *A. japonicus*

Following the *in vitro* characterization of AjSK/CCKs, we investigated their *in vivo* effects on *A. japonicus*. We found that, compared to the normally fed control group, the expression levels of *AjSK/CCKP* in CNR and intestine of *A. japonicus* were significantly reduced following food deprivation, and the reduction was reversed upon refeeding **(Fig. 6A)**. Subsequently, we conducted a 25-day *in vivo* injection experiment to assess the effects of AjSK/CCK1 and AjSK/CCK2 on feeding and growth in *A. japonicus*. The results demonstrated that chronic injection of either AjSK/CCK1 or AjSK/CCK2 significantly reduced the weight gain rate (WGR), specific growth rate (SGR), and feeding rate (FIR) in *A. japonicus* relative to the control group. Notably, AjSK/CCK2 exerted a stronger inhibitory effect on feeding and growth than AjSK/CCK1 **(Fig. 6B)**. Correspondingly, compared with the control group, the AjSK/CCK1-injected group showed a significant increase in remaining bait at stage V and a significant decrease in excrement at stages IV and V. In the AjSK/CCK2-injected group, remaining bait was significantly increased at stages II, III, IV, and V, while excrement was significantly decreased at stages III, IV, and V **(Fig. 6C)**. Intestinal contents appeared to be decreased compared with the control group after long-term injection of AjSK/CCK1 and AjSK/CCK2 **(Additional file 1: Fig. S6)**.

To further elucidate the molecular mechanisms underlying inhibition on feeding of AjSK/CCK1 and AjSK/CCK2, we examined the expression of *AjOrexin1P* and *AjOrexin2P*, which produce two orexin peptides and are co-expressed with *AjSK/CCKR* in the peptidergic

neuron type 3 (47). The results showed that, compared with the control group, the AjSK/CCK1-injected group exhibited significantly downregulated expression of *AjOrexin1P* in CNR, as well as *AjOrexin1P* and *AjOrexin2P* in intestine. In the AjSK/CCK2-injected group, significant downregulation was observed for *AjOrexin1P* and *AjOrexin2P* in the CNR and intestine **(Fig. 6D)**. To further explore the effects of AjSK/CCK1 and AjSK/CCK2 on growth in *A. japonicus*, we analyzed the expression of several growth-related factors, including multiple epidermal growth factor 6 (*AjMegf6*, GenBank accession number: MG018199.1), insulin-like growth factor (*AjIgf*, GenBank accession number: PIK50518.1) and growth and differentiation factor-8 (*AjGDF-8*, GenBank accession number: KP100064.1) in intestine after AjSK/CCK1 and AjSK/CCK2 injection (48-50). We found that *AjGDF-8*, an inhibitory factor for muscle development and growth in vertebrates, was significantly up-regulated in intestine of *A. japonicus* after injection of AjSK/CCK1 and AjSK/CCK2 (49, 51). However, *AjMegf6* and *AjIgf* showed no significant changes in expression compared with the control group **(Fig. 6E)**.

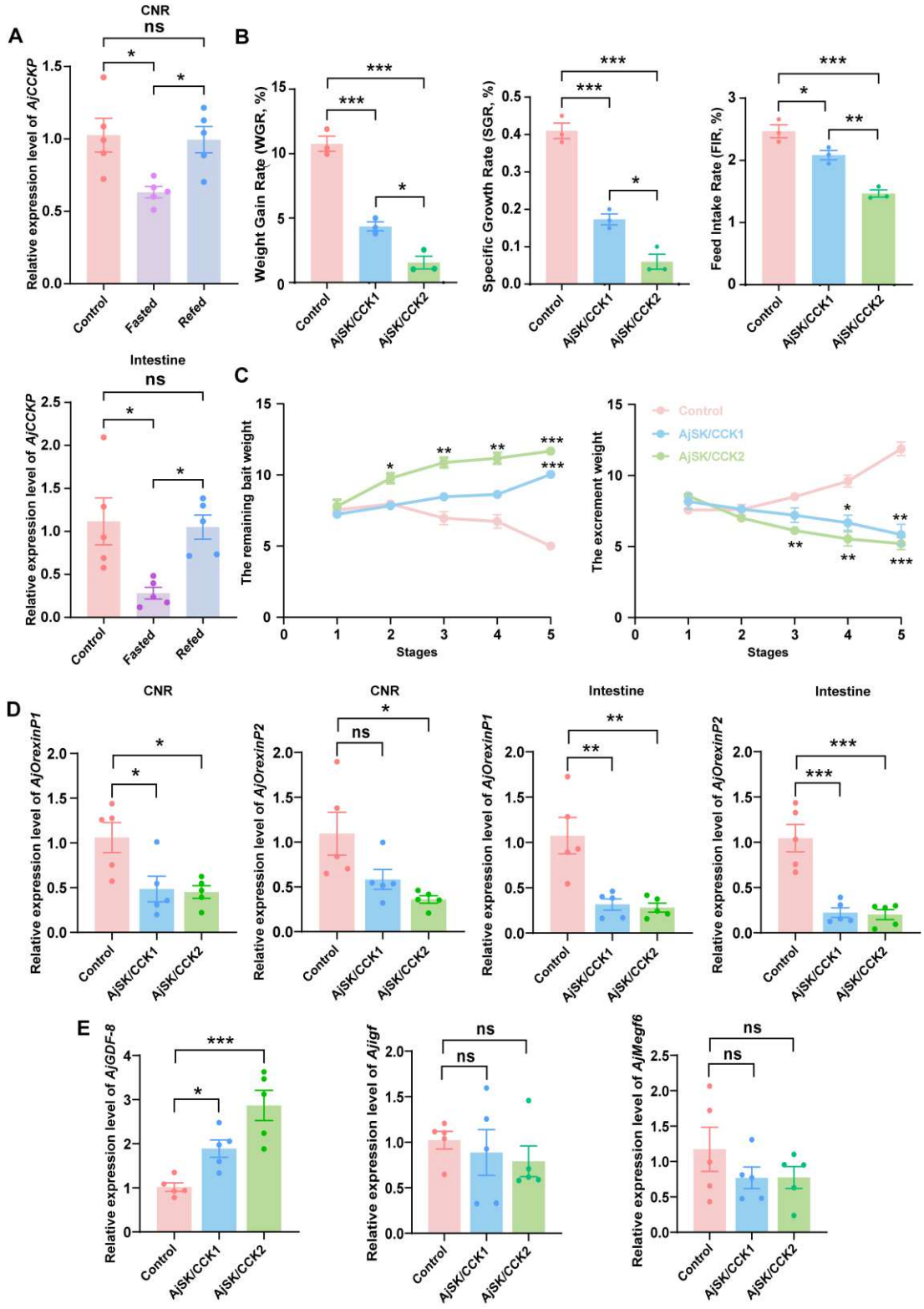

Figure 6. The effects of AjSK/CCK1 and AjSK/CCK2 on feeding and growth in *A. japonicus*

A. The expression levels of *AjSK/CCKP* are significantly different between control animals and fasted animals and between fasted animals and fasted animals after refeeding in CNR ($F_{(2,}$

$_{12)}$=6.167) and intestine ($F_{(2, 12)}$=6.528) (n=5). **B**. WGR ($F_{(2, 6)}$=94.85), SGR ($F_{(2, 6)}$=91.61), FIR ($F_{(2, 6)}$=38.44) after long-term injection of AjSK/CCK1 and AjSK/CCK2 (n=3). **C**. The remaining bait weight (treatment: ($F_{(2, 6)}$=116.5)) and excrement weight (treatment: ($F_{(2, 6)}$=38.61)) at different stages (Ⅰ−Ⅴ) of a 25-day injection experiment (n=3). **D**. The relative expression levels of *AjOrexinP1* (CNR: $F_{(2, 12)}$=6.615, intestine: $F_{(2, 12)}$=13.01) and *AjOrexinP2* (CNR: $F_{(2, 12)}$=5.94, intestine: $F_{(2, 12)}$=24.24) in CNR and intestine (n=5). **E**. The relative intestinal expression levels of *AjGDF-8* ($F_{(2, 12)}$=15.47), *AjIgf*, *AjMegf6* (n=5). Asterisks represent significant differences as follows: *: $p \leq 0.05$, **: $p \leq 0.01$, ***: $p \leq 0.001$, ns: no significant difference.

Discussion

Molecular characterisation of SK/CCK-type neuropeptide signaling in the sea cucumber *A. japonicus*

The SK/CCK-type neuropeptide signaling system in *A. japonicus* comprises a precursor protein that gives rise to two mature peptides, AjSK/CCK1 and AjSK/CCK2, both featuring conserved structural characteristics of this neuropeptide family: a tyrosine residue predicted to be sulphated post-translationally and a C-terminally amidated aromatic amino acid, as well as a corresponding SK/CCK-type receptor (8, 13, 37). In *A. japonicus*, as in other echinoderms, the SK/CCK-type peptides are typically located near the C-terminal region of SK/CCK-type precursor protein, whereas the number of SK/CCK-type neuropeptides varies among classes: two in Holothuroidea (sea cucumbers) and Asteroidea (starfish), three in Echinoidea (sea urchins) and Ophiuroidea (brittle stars), and one in Crinoidea (13, 52-55). A comparable pattern of variation is observed in arthropods: most insects typically have two SK/CCK-type neuropeptides; however, three are found in the shrimp *Penaeus monodon* and the giant springtail *Tetrodontophora bielanensis*, while only one is present in *Locusta migratoria*, *Bombyx mori* and *Manduca sexta* (8, 56-58).

SK/CCK-type neuropeptides typically bind to G protein-coupled receptors (GPCRs) to exert their effects, and one candidate receptor for SK/CCK-type neuropeptides was identified in *A. japonicus*, whereas two receptors have been identified in most chordates and mollusks and

three receptors in nematodes (4, 26, 28, 32, 59). Phylogenetic analysis supports the existence of a single SK/CCK-type receptor gene in a common ancestor of the Bilateria, with lineage-specific duplications/deletions leading to receptor number variation (37). To functionally validate the candidate receptor for AjSK/CCK1 and AjSK/CCK2, we conducted receptor activation assays using HEK293T cells expressing AjSK/CCKR and G5A protein. Results showed that both AjSK/CCK1 and AjSK/CCK2 exhibited comparable potency as ligands for AjSK/CCKR, with EC_{50} values of 2.06 nM and 3.92 nM, respectively. However, AjSK/CCK2 exhibited higher maximal efficacy than AjSK/CCK1 as a ligand for AjSK/CCKR. The potency of AjSK/CCKR for the non-sulfated peptides AjSK/CCK1ns and AjSK/CCK2ns is relatively low, with EC_{50} values of 2.33 μM and 7.72 μM, respectively. This characteristic of AjSK/CCKR is consistent with the properties of many SK/CCK-type receptors in other taxa, including CCKR1 in mammals, DSK-R1 in *Drosophila melanogaster*, apCCKR1 and apCCKR2 in *Aplysia californica* (4, 32, 60). However, sulfation is not a universal requirement for SK/CCK-type receptor activation, and non-sulphated SK/CCK-type peptides can function as potent agonists for CCKR2 in mammals and for both CKR2a and CKR2b in the nematode *Caenorhabditis elegans* (26, 32). In addition, AjSK/CCK1 and AjSK/CCK2 both activate the Gαq/Ca^{2+}/PKC signaling cascade and downstream ERK1/2 phosphorylation, which is consistent with the classic signaling mechanism of SK/CCK receptors primarily coupling to Gq/11 proteins (30, 45, 60). However, neither peptide activated the cAMP/PKA pathway, although SK/CCK receptors have been reported to couple to Gs proteins in some species (26, 61).

As AjSK/CCK2 exhibited stronger efficacy than AjSK/CCK1 in receptor activation, this prompted us to investigate the structural basis of their interaction with AjSK/CCKR through molecular docking. We found that the AjSK/CCK1-AjSK/CCKR and AjSK/CCK2-AjSK/CCKR complexes exhibited comparable binding energies, −9.7 kcal/mol and −9.3 kcal/mol, respectively. However, their binding modes differed significantly: AjSK/CCK1 contains a C-terminal tri-phenylalanine motif, whose hydrophobic side chains mediate extensive hydrophobic contacts, whereas AjSK/CCK2 carries a hydrophilic methionine at the third position of the C-terminus, enabling the formation of more specific and directed hydrogen bonds with key residues in the receptor binding pocket, which may stabilize the active conformation of the receptor more effectively and promote more efficient downstream signaling (62-64).

Physiological characterisation of SK/CCK-type neuropeptide signaling in the sea cucumber *A. japonicus*

Having characterized the SK/CCK-type neuropeptide signaling system in *A. japonicus* at the molecular level, we next focused on investigating its physiological roles in this species. We found that *AjSK/CCKP* and *AjSK/CCKR* both have broad expression patterns, and the highest level of expression was detected in the intestine of *A. japonicus*, suggesting potential roles in multiple physiological processes of the digestive system.

Based on the expression of *AjSK/CCKP* and *AjSK/CCKR* in the longitudinal muscle and digestive tissues of *A. japonicus*, we prepared *in vitro* muscle preparations from these tissues, including the longitudinal muscle, esophagus, anterior and posterior intestine, to test the pharmacological effects of AjSK/CCK1 and AjSK/CCK2. We found that both AjSK/CCK1 and AjSK/CCK2 induced concentration-dependent contraction of the longitudinal muscle in *A. japonicus*. In accordance with this finding, SK/CCK-type peptides cause contraction of the body wall-associated apical muscle in the arms of starfish *A. rubens* (13). Furthermore, expression of an SK/CCK-type peptide is detected in nerve fibres innervating the tourniquet muscle, which mediates constriction of the arm during and after the process of autotomy in *A. rubens* (65). In sea cucumbers, the alternating contraction/relaxation of longitudinal muscles of the body wall constitutes a fundamental basis for locomotion (66). Thus, SK/CCK-type neuropeptides may have a general role in echinoderms in regulating body wall shape, posture, and locomotion. In addition, AjSK/CCK2 also elicited sustained contraction of the posterior intestine, but it had no effect on esophagus or anterior intestine preparations. These location-dependent effects of SK/CCK-type peptides highlight their capacity for complex, segment-specific regulation of the digestive tract, which allows precise control over intestinal motility patterns.

Having investigated the *in vitro* effects of SK/CCK-type peptides in *A. japonicus*, we then investigated their *in vivo* effects on feeding and growth in *A. japonicus* and found that chronic administration of either AjSK/CCK1 or AjSK/CCK2 significantly suppressed WGR, SGR, and FIR, with AjSK/CCK2 exhibiting a more pronounced inhibitory effect. This was accompanied by a marked increase in remaining bait accumulation and a decrease in excrement output compared to the control group. Thus, a consistent finding of this study at the level of the receptor

protein AjSK/CCKR, tissues/organs and the whole-animal is that AjSK/CCK2 has higher potency/efficacy than AjSK/CCK1. As discussed above, this could be attributed to differences in molecular interaction of the two peptides with AjSK/CCKR. However, differences in potency/efficacy at the level of tissues/organs and the whole-animal may also be attributable to other consequences of differences in the physicochemical properties of the two peptides. Specifically, the C-terminal region of AjSK/CCK1 consists of three consecutive strongly hydrophobic phenylalanine (F) residues, whereas this motif is interrupted by a methionine (M) in AjSK/CCK2. This structural variation is predicted to confer higher solubility to AjSK/CCK2, as supported by their Grand Average of Hydropathy (GRAVY) values: −0.100 for AjSK/CCK2 vs +0.344 for AjSK/CCK1. A consequent difference in solubility may therefore influence their tissue permeability and thereby contribute to the observed differences in potency/efficacy *in vitro* and *in vivo*.

In conclusion, the inhibitory effect of AjSK/CCK1 and AjSK/CCK2 on feeding and growth in *A. japonicus* are aligned with findings in other bilaterians (8, 12, 13). Critically, the position of echinoderms as a phylogenetic 'intermediate' between protostomes and chordates offers a unique comparative vantage point, which provides crucial evidence for the ancestral role of SK/CCK-type neuropeptides as feeding regulators across the Bilateria.

Comparative physiology and evolution of SK/CCK-type neuropeptide signaling as a regulator of feeding related processes.

SK/CCK-type neuropeptides exhibit conserved myomodulatory effects, especially on digestive tract muscles, across both deuterostomes and protostomes. A previous study reported that mammalian CCK-8 induced relaxation of intestine preparations in the sea cucumber *Holothuria glaberrima in vitro* (67), whereas we found that SK/CCK-type neuropeptides in *A. japonicus* triggered sustained contraction of the posterior intestine, which aligns with the action of SK/CCK-type neuropeptides in triggering cardiac stomach contraction in the starfish *A. rubens* (13). It is possible, therefore, that the relaxing effect of CCK-8 on intestine preparations in the sea cucumber *H. glaberrima* is not physiologically relevant and may be due to interaction of CCK-8 with receptors for other types of neuropeptides in this species.

Numerous studies have reported that SK/CCK-type peptides modulate intestinal motility, with location-dependent effects on contraction patterns **(Fig. 7)**. For example, in the ballan wrasse *Labrus berggylta*, CCK reduced propagating contractions in the anterior part of intestine, but increased both non-propagating and propagating contractions in the posterior part of intestine (68). Similarly, in the oyster *Crassostrea gigas* (now known as *Magallana gigas*), Cragi-CCK1 decreased the frequency of hindgut spontaneous contractions, while in the goldfish *Carassius auratus*, CCK evoked proximal intestine contractility (28, 69). Here, we found that AjSK/CCK2 induced contraction of the posterior intestine from *A. japonicus*, but it had no observable effects on esophagus and anterior intestine, even though the esophagus preparations display greater contractility as evidenced by stronger contraction responses to acetylcholine (ACh) (70). The primary reported action of CCK in vertebrate digestive systems is inhibition of gastric emptying through relaxation of the gastric fundus and contraction of the pyloric sphincter (7, 19, 71). In most vertebrates, the stomach is anatomically divided into two regions: the proximal cardiac stomach and the distal pyloric stomach, and the pyloric region gradually narrows into the pyloric sphincter, which, together with the intestinal entrance, creates resistance to inhibit the passage of chyme from the stomach into the intestine (72, 73). The digestive tract of sea cucumbers is divided into the following parts: the pharynx, esophagus, stomach, intestine (anterior, middle and posterior part), and cloaca, based on fine-scale structural characteristics (66, 74). However, in sea cucumbers, the transitional region between the stomach and intestine, termed the "transition zone" as described by Kamenev et al. (2013), features a notably thinner muscular layer, indicating this region may lack the functional capacity to impede the passage of food into the intestine (74). On the other hand, the posterior intestine opens into the cloaca through a narrow orifice that is kept tightly closed by an intestinal sphincter (66). Therefore, we propose that SK/CCK-type neuropeptides in *A. japonicus* inhibit intestinal emptying and ultimately reduce food intake primarily by inducing sustained contraction of the posterior intestine, rather than by acting on other regions of the digestive tract. Furthermore, we found that *AjSK/CCKP* expression in the intestine of *A. japonicus* significantly increased after feeding, which aligns with a conserved regulatory logic but targeting distinct anatomical sites to those in mammals. Thus, in mammals, CCK contracts the pyloric sphincter to prolong retention in the enzymatic stomach, whereas in sea cucumbers, the

esophagus and stomach function primarily in transport and mechanical processing, and digestion occurs in the anterior and middle intestine, so SK/CCK-type peptides accordingly induce contraction of the posterior intestine to serve a similar purpose (75-77). This divergence underscores the adaptive evolution of SK/CCK-type neuropeptide signaling system function: it exerts an ancient feeding inhibitory function through a similar mechanical regulatory mechanism, while the specific anatomical targets of its action have diversified due to structural differences in the digestive tract across species.

Inhibition of digestive tract emptying cannot fully account for the inhibitory effects of SK/CCK-type neuropeptides on feeding. For instance, in rats with open gastric fistulas, exogenous administration of CCK still elicited a full behavioral sequence of satiety (78). Similarly, our study found that chronic injection of AjSK/CCK1, which had no myomodulatory effect on the posterior intestine, significantly suppressed both feeding and growth of *A. japonicus*, albeit less potently than AjSK/CCK2. Orexin-type neuropeptides, which are conserved orexigenic factors in many vertebrates, are known to interact with SK/CCK-type signaling to regulate feeding behavior (79-81). In rats, CCK infusion suppresses prepro-orexin mRNA expression and orexin-A pretreatment abolishes CCK-induced feeding inhibition (82, 83). In *A. japonicus*, two orexin-type neuropeptide precursors have been identified and here we found that long-term AjSK/CCK1 and AjSK/CCK2 injection significantly down-regulated *AjOrexinP1* and *AjOrexinP2* expression in the intestine and CNR of *A. japonicus*. And orexin is known to promote feeding both centrally (by stimulating appetite) and peripherally (by modulating gut motility and digestive enzyme secretion), this downregulation suggests that inhibition of orexin signaling may contribute to the anorexic effect of SK/CCK-type neuropeptides (54, 81). In conclusion, the conserved interaction between the SK/CCK-type and orexin-type neuropeptide signaling systems across species highlights a key evolutionary principle. Furthermore, while the anatomical targets of some neuropeptides diversify with physiological structures, certain core regulatory networks within organisms maintain remarkable stability.

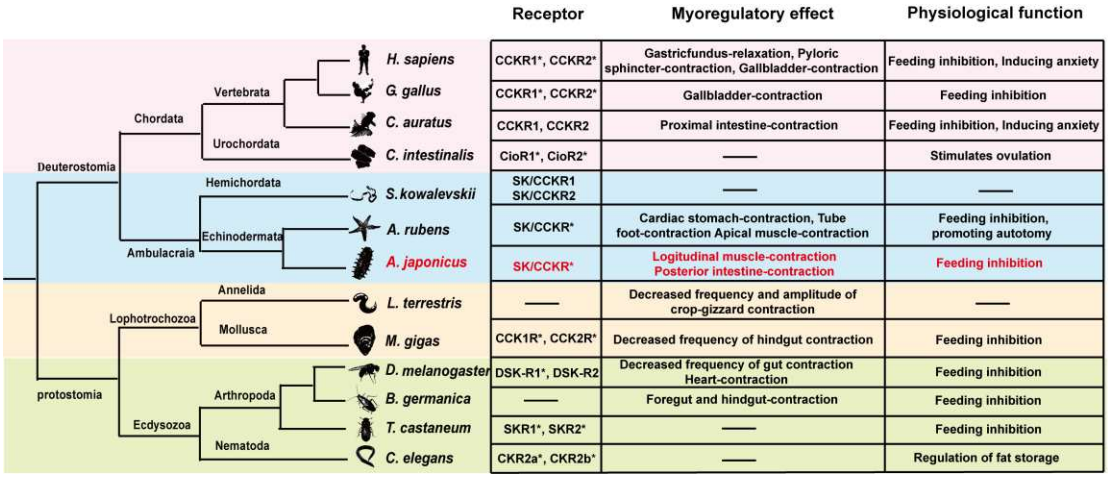

Figure 7. Receptor identification, myoregulatory effects and physiological functions of SK/CCK-type neuropeptides in representative bilaterian species

Species are classified by different colors: pink, Chordata; blue, ambulacraia; yellow, lophotrochozoa; green, ecdysozoa. The dash (−) indicates that no relevant studies have been reported and the asterisk (*) indicates that ligand-receptor activation assays have been performed.

Conclusions

In summary, we have characterized the SK/CCK-type neuropeptide signaling system in a deuterostome invertebrate, the sea cucumber *A. japonicus*, including its molecular properties, expression profile, *in vitro* pharmacological effects and *in vivo* physiological actions. A single SK/CCK-type precursor in *A. japonicus* generates two mature SK/CCK-type neuropeptides: AjSK/CCK1 and AjSK/CCK2, which both exhibit an evolutionarily conserved role in inhibiting feeding and growth. We propose that SK/CCK-type neuropeptides suppress feeding and growth in *A. japonicus* through dual mechanisms: neurologically, AjSK/CCK1 and AjSK/CCK2 reduce appetite by down-regulating expression of orexin-type neuropeptides in the central nervous system, leading to decreased food intake. Mechanistically, AjSK/CCK2 induces sustained contraction of the posterior intestine, thereby inhibiting intestinal emptying and decreasing food intake. Taken together, this study not only confirms the evolutionary conservation and adaptability of SK/CCK-type neuropeptide in feeding-regulating mechanisms across invertebrates and vertebrates, but it also provides theoretical insights for improving aquaculture of *A. japonicus*, a commercially important species. For example, development of

AjSK/CCKR antagonists could provide a novel strategy for promoting feeding and growth in *A. japoncius*.

Methods

Animals

Adult sea cucumbers (*A. japonicus*) were collected from a commercial farm in Qingdao, China (119.90752° E, 35.64737° N). The animals were placed on ice and transported to the laboratory by truck within 2 h. Prior to experiments, they were acclimatized in laboratory aquaria for one week under controlled conditions (salinity: 32 ppt; dissolved oxygen: 8 mg/L; temperature: 15 °C), and fed daily with a formulated commercial feed containing kelp, scallop skirt, brown alga (*Sargassum thunbergii*), gulfweed, Ulva and yeast. For reverse transcription-quantitative real-time polymerase chain reaction (RT-qPCR) analysis, CNR, intestine, longitudinal muscle, respiratory tree, and gonad were dissected from five individuals and stored at −80°C. For *in vitro* pharmacological assays, longitudinal muscle strips, esophagus preparations, anterior and posterior intestine preparations were dissected from fifty adults (100g–120g). Fifteen and ninety individuals (32.8 ± 4.8 g) were used for food deprivation experiments and *in vivo* studies, respectively.

Cloning and sequence analysis of cDNAs encoding the *A. japonicus* SK/CCK-type precursor

A full-length cDNA encoding the AjSK/CCK-type precursor was amplified via High-Fidelity PCR (Vazyme, Cat No. P505) using sequence-specific primers, and then the PCR product was purified, sequenced, and analyzed. The open reading frame (ORF) and corresponding amino acid sequence were identified using bioinformatic tools (http://www.bio-soft.net/sms/index.html). The tertiary structure of the precursor was modeled using SWISS-MODEL (https://swissmodel.expasy.org/interactive). For comparative analysis, SK/CCK-type precursor sequences from other bilaterians were obtained and GSDS 2.0 (http://gsds.gao-lab.org/index.php) was used to predict gene structure. MEGA7 (v.7170509) with default parameters was used for multiple sequence alignment, and GeneDoc v.2.7

(https://genedoc.software.informer.com/) was used for editing. The Grand Average of Hydropathy (GRAVY) values for mature peptides were calculated using ProtParam (https://web.expasy.org/protparam/). Sequence relationships were analyzed across bilaterians using the CLANS clustering method with a BLAST-based comparison (BLOSUM62, e-value≤1e-2). The specific primers are listed in **Additional file 4: Dataset S3**.

Identification of a candidate *A. japonicus* SK/CCK receptor

Using the SK/CCK-type receptor of *A. rubens*, which has been characterized pharmacologically, as the query sequence, one transcript encoding an SK/CCK-type receptor was identified by tBLASTn analysis of *A. japonicus* CNR transcriptome data (13). The full-length cDNA of AjSK/CCKR was amplified by High-Fidelity PCR using specific primers **(Additional file 4: Dataset S3)** and the PCR product was purified and sequenced. Phylogenetic analysis of SK/CCKRs in bilaterians was performed on the aligned receptor sequences, which were downloaded from NCBI and conducted with MAFFT v7.526 using the L-INS-i algorithm and a maximum of 1000 iterative refinement steps to optimize alignment accuracy (84). The resulting alignment was subsequently trimmed using trimAl v1.4.rev15 under the “automated1” heuristic method to remove regions of low quality or uncertain homology (85). A maximum-likelihood phylogenetic tree was then inferred using IQ-tree v3.0.1 for Linux x86 64-bit, with the best-fit substitution model automatically selected via the ModelFinder Plus (MFP) procedure (1000 bootstrap replicates) (86, 87). The resulting tree was rooted using deuterostome orexin-type receptors as the outgroup and visualized using the online website iTOL.

Using the same methods employed for AjSK/CCKP, the ORF region, the corresponding amino acid sequence and the tertiary structure of AjSK/CCKR were analyzed. Furthermore, the seven transmembrane domains and putative phosphorylation sites of AjSK/CCKR were predicted using Protter 1.0 (http://wlab.ethz.ch/protter/start/) and NetPhos-3.1 (https://services.healthtech.dtu.dk/service.php?NetPhos-3.1), respectively **(Additional file 1: Fig. S2)**. The accession numbers of the protein sequences employed in the phylogenetic analysis are listed in **Additional file 3: Dataset S2**.

Pharmacological characterization of AjSK/CCKR

To test whether AjSK/CCK1 and AjSK/CCK2 act as ligands for AjSK/CCKR, the complete ORF of AjSK/CCKR with a Kozak sequence (ACC) before the ATG was synthesized by High-Fidelity PCR and cloned into the pcDNA3.1(+) vector (Biofeng, Cat. No. V790-20) using Trelief SoSoo Cloning Kit (QINGKE, Cat. No. TSV-S1). The primers used for plasmid construction are listed in **Additional file 4: Dataset S3**. HEK293T cells (Procell, CL-0005) were cultured at 37°C with 5% CO_2 atmosphere in Dulbecco's Modified Eagle's Medium (DMEM) (Biosharp, Cat. No. BL304A) supplemented with 10% fetal bovine serum (FBS) and then cells were transferred into clear bottom 96-well plates to grow for two days. At about 90% confluency, cells were co-transfected with AjSK/CCKR plasmid and the calcium-sensitive bioluminescent reporter GFP-aequorin fusion protein (G5A) plasmid using Lipofectamine 2000 (Thermo Fisher Scientific, Cat. No. 11668-027). For each well, 20 µl OptiMEM, 100 ng of AjSK/CCKR plasmid, 100 ng of G5A plasmid (to produce luminescence after the receptor is activated) and 0.45 µl lipofectamine 2000 were mixed and incubated for 20min. Then, the transfection mixture was added to wells. Two days post-transfection, the medium in each well was removed and substituted with 100 µl OptiMEM medium supplemented with 4 µM coelenterazine-H (Rhawn, R030699). After an incubation period of 2-3 h, the medium was removed and cells were exposed to 100 µl OptiMEM medium containing different concentrations (10^{-14} M to 10^{-4} M, gradient method for dilution) of synthetic AjSK/CCK1: DY(SO_3)GDLGFFF-NH_2 or AjSK/CCK2: DY(SO_3)NDLGMFF-NH_2 (custom synthesized by Sangon Biotech, China, purity>95%) in clear bottom 96-well plates. In parallel, the non-sulphated peptide variants, AjSK/CCK1ns (DYGDLGFFF-NH_2) and AjSK/CCK2ns (DYNDLGMFF-NH_2) were applied under identical conditions to assess the functional contribution of tyrosine sulphation to receptor activation. Luminescence in each well was measured using a Synergy H1 Hybrid Multi-Mode Reader (Biotek, America) for a period of 30 seconds and each time a single well was recorded. Each concentration was tested in three independent experiments with triplicates, and the average of the triplicates from each experiment was used for normalization. Responses were normalized relative to the maximum response (set as 100% activation) and the vehicle control response (set as 0% activation) within each experiment. Dose-response curves were fitted using a four-parameter logistic model, and EC_{50} values were derived as the concentration eliciting 50% of the maximal response.

Subsequently, to investigate which signaling pathway was activated by AjSK/CCKR, we

conducted SRE/CRE (Serum-responsive element/cAMP response element)-Luc (Luciferase) detection and Western blotting. SRE-Leu and CRE-Leu are specific reporter systems for monitoring the activation of protein kinase C (PKC) and protein kinase A (PKA), respectively (41). For SRE/CRE-Luc detection assays, after 48 h of expression, HEK293T cells co-transfected with *AjSK/CCR*/pcDNA 3.1(+) and pSRE/pCRE-Luc were incubated with different concentrations of AjSK/CCK1 or AjSK/CCK2 (10^{-14} M-10^{-4} M) for 4h at 37°C. A firefly luciferase reporter gene assay kit (MK, MF4001) was used following the manufacturer's instructions to detect SRE/CRE luciferase activity. Each concentration was tested in three independent experiments with triplicates, and the average of the triplicates from each experiment was used for curve fitting. HEK293T cells co-transfected with empty pcDNA3.1(+) vector and pSRE/pCRE-Luc were used as negative controls. For Western blotting, HEK293T cells transfected with *AjSK/CCR*/pcDNA 3.1(+) were starved in serum-free DMEM for 2 hours after 48 hours of expression. The cells were then stimulated with 10^{-6} M AjSK/CCK1 or AjSK/CCK2 for the indicated times (0, 5, 15, 30, 45, and 60min), and the band intensity at 0 min (without neuropeptide stimulation) was used as the control. Following blocking with 5% BSA (G-CLONE, PN0011), PVDF membranes containing proteins (0.05mg) extracted from the cells were incubated overnight with anti-phospho-ERK1/2 antibody (T202/Y204, rabbit monoclonal, 1:2000) or anti-ERK1/2 antibody (rabbit monoclonal, 1:2000) (Cell Signaling Technology, Cat. No. 4370, 4695), then with a horseradish peroxidase-conjugated goat anti-rabbit IgG secondary antibody (goat polyclonal, 1:2000) (Absin, abs20040), and finally detected using Omni-ECL™ Femto Light chemiluminescent reagents (EpiZyme, SQ201) on an RVL-100-G imaging system (ECHO, America). Three independent experimental replicates were performed for both AjSK/CCK1 and AjSK/CCK2.

Molecular docking of AjSK/CCKs with AjSK/CCKR

To elucidate potential interactions between AjSK/CCKs and AjSK/CCKR, the three-dimensional (3D) structures of both ligands and receptor were predicted using AlphaFold3 (https://alphafoldserver.com) (88). The highest-confidence models, selected based on per-residue confidence scores (pLDDT), were used for subsequent molecular docking studies. Prior to docking, the receptor and ligand structures were prepared using AutoDockTools v1.5.6,

including the addition of polar hydrogen atoms and assignment of Gasteiger charges, and were subsequently converted into .pdbqt format (89). AutoDock Vina v1.2.2 was used to perform semi-flexible docking, which allows the ligands to sample various conformations while keeping the receptor rigid (90). The interaction interface residues were defined in the three-dimensional grid (x = 0.397, y = −12.544, z = −25.268) while the grid dimension was 40 × 40 × 40 with the exhaustiveness set to 8. The resulting poses were ranked by binding affinity, and the lowest-energy conformation for each complex was retained for further analysis. Then, the refined docking models were subjected to 3D visualization in PyMOL v4.6.0 and annotated with LigPlot+ v2.3.1 (91) to facilitate detailed characterization of the binding interfaces between AjSK/CCKs and AjSK/CCKR.

Analysis of the organ/tissue expression profile of AjSK/CCKP and AjSK/CCKR

For expression analysis of AjSK/CCKP and AjSK/CCKR, total RNA was isolated from five organs/tissues (CNR, intestine, longitudinal muscle, respiratory tree and gonad) of five individuals using Trizol RNA isolation reagent (Vazyme, Cat. No. R401-01) following the manufacturer's instructions. A total of 500 ng RNA was reverse transcribed to cDNA by Hifair® III 1st Strand cDNA Synthesis SuperMix (Yeasen, Cat. No. 11141ES60). The amplification for RT-qPCR was performed in 15 μL volume reactions using Hieff UNICON Universal Blue qPCR SYBR Green Master Mix (Yeasen, Cat No. 11184ES08) and the Corbett Rotor-Gene Q (Qiagen, Germany) were applied to assess the expression levels of *AjSK/CCKP* and *AjSK/CCKR*. *β-actin* (GenBank accession number: PIK61412.1) and *β-tubulin* (GenBank accession number: PIK51093) were used as housekeeping genes for standardization in accordance with a previous study (92). The $2^{-\Delta\Delta CT}$ method was used to analyze the relative expression levels. The specific primers for RT-qPCR analysis of *AjSK/CCKP* and *AjSK/CCKR* expression are listed in **Additional file 4: Dataset S3**.

***In vitro* pharmacological effects of AjSK/CCK1 and AjSK/CCK2**

To investigate the effects of these peptides on myoactivity, including sulphated peptides (AjSK/CCK1, AjSK/CCK2) and non-sulphated peptides (AjSK/CCK1ns, AjSK/CCK2ns), preparations of the longitudinal muscle, esophagus, anterior and posterior intestine dissected

from adult *A. japonicus* were prepared. Briefly, the longitudinal muscle, esophagus, anterior and posterior intestine of *A. japonicus* were dissected and cut into strips approximately 20 mm in length. These preparations were set up in a 50 ml glass chamber containing 30 ml sterilized seawater at about 15°C, with one end tied to a metal hook at the bottom and the other end tied to a High Grade Isotonic Transducer (ADinstruments MLT0015, Oxford, UK) connected with PowerLab data acquisition hardware (ADinstruments PowerLab 4/26, Oxford, UK) via cotton threads. LabChart (v8.0.7) software was used to record the output signal (cm) from the isotonic transducer. Prior to testing, the preparations were equilibrated for at least 20min with 0.5 g resting tension. When the muscle preparations reached a stable baseline state, 30 μl peptide dissolved in PBS with 1% DMSO (to aid solubility) was added into the organ bath to achieve different concentrations (longitudinal muscle, 10^{-9} M to 10^{-6} M; anterior and posterior intestine, 10^{-9} M to 10^{-5} M). Each concentration was tested in triplicate with preparations from different individuals, and the same volume of PBS with 1% DMSO was added as a negative control.

***In vivo* pharmacological effects of AjSK/CCK1 and AjSK/CCK2**

For a food deprivation experiment, 15 sea cucumbers were evenly divided into three experimental groups: a control group (fed daily), a fasted group (subjected to 14 days of food deprivation), and a refed group (fasted for 14 days followed by refeeding), and CNR and intestine were collected at the end of the experimental period for subsequent RT-qPCR analysis. In the refed group, sampling was performed 24 hours after food was reintroduced. For a 25-day long-term injection experiment, 90 sea cucumbers were evenly divided into three groups (AjSK/CCK1, AjSK/CCK2, and control group) randomly. Then 30 sea cucumbers in each group was randomly divided into three seawater tanks with 10 in each tank. Peptides were dissolved in PBS with 1% DMSO to a final concentration of 0.5 mg/ml as previously reported and injected into the coelom via the tentacles (11, 16). The peptide solution was injected once every 2 days at noon with 1 μl/g wet weight, and an equal volume of PBS containing 1% DMSO was used as the control group. The wet weight of each individual was measured at the beginning and after 25 days injection. Each tank was provided daily with a sufficient diet and the remaining bait and excrement from each tank were collected, dried, and weighed daily. The WGR, SGR and FIR of each group were calculated using formulas as previously described

(93).

After injection, the intestines and CNRs from sea cucumbers in the AjSK/CCK1, AjSK/CCK2 and control groups were collected and stored at −80°C for analysis of gene expression using RT-qPCR and employing the same experimental procedure as described above. Orexin-type neuropeptides are regulators of feeding that promote feeding in a variety of species, and two orexin-type neuropeptide precursors (*AjOrexin1P*, GenBank accession numbers: MF401988; *AjOrexin2P*, GenBank accession numbers: MF401989) have been identified in *A. japonicus* (54, 81). Therefore, the expression levels of *AjOrexin1P* and *AjOrexin2P* were assessed by RT-qPCR to investigate potential cross-regulation between SK/CCK-type and orexin-type signaling in association with control of feeding in *A. japonicus*. Expression of several growth factor genes, including multiple epidermal growth factor 6 (*AjMegf6*, GenBank accession number: MG018199.1), insulin-like growth factor (*AjIgf*, GenBank accession number: PIK50518.1) and growth and differentiation factor-8 (*AjGDF-8*, GenBank accession number: KP100064.1), was investigated to explore potential effects of AjSK/CCK1 and AjSK/CCK2 on growth-related processes in *A. japonicus* (49, 50, 94).

Statistical analysis

All statistical analyses were performed using GraphPad Prism 8.0, and data are presented as mean ± SEM from at least three independent biological replicates. For comparisons among multiple groups, one-way ANOVA followed by Tukey's multiple comparison test was applied to ERK1/2 phosphorylation levels, WGR, SGR, FIR, and all RT-qPCR gene expression data. Differences in maximal receptor activation efficacy between AjSK/CCK1 and AjSK/CCK2 were assessed using two-tailed Student's *t-test*. For pharmacological assays (longitudinal muscle contraction) and functional experiments (remaining bait and excrement weight), two-way ANOVA with Greenhouse-Geisser correction was used to evaluate differences between peptides. Significance levels denoted as *: $p \leq 0.05$, **: $p \leq 0.01$ and ***: $p \leq 0.001$ in the figures. Dose-response curves were fitted by nonlinear regression based on a four-parameter logistic model with automatic outlier exclusion, and half-maximal effective concentration (EC_{50}) values were calculated using the built-in algorithms of GraphPad Prism 8.0.

Abbreviations

ACh: acetylcholine

Aj: Apostichopus japonicus

AjGDF-8: Apostichopus japonicus growth and differentiation factor-8

AjIgf: Apostichopus japonicus insulin-like growth factor

AjMegf6: Apostichopus japonicus multiple epidermal growth factor 6

AjOrexin1P: Apostichopus japonicus orexin 1 precursor

AjOrexin2P: Apostichopus japonicus orexin 2 precursor

AjSK/CCK1: Apostichopus japonicus sulfakinin/cholecystokinin 1

AjSK/CCK1ns: Apostichopus japonicus sulfakinin/cholecystokinin 1 non-sulphated

AjSK/CCK2: Apostichopus japonicus sulfakinin/cholecystokinin 2

AjSK/CCK2ns: Apostichopus japonicus sulfakinin/cholecystokinin 2 non-sulphated

AjSK/CCKP: Apostichopus japonicus sulfakinin/cholecystokinin precursor

AjSK/CCKR: Apostichopus japonicus sulfakinin/cholecystokinin receptor

apCCKR1: Aplysia californica cholecystokinin receptor 1

apCCKR2: Aplysia californica cholecystokinin receptor 2

cAMP: cyclic adenosine monophosphate

CCK: cholecystokinin

CKR1: Caenorhabditis elegans sulfakinin receptor 1

CKR2a: Caenorhabditis elegans sulfakinin receptor 2a

CKR2b: Caenorhabditis elegans sulfakinin receptor 2b

CNR: circumoral nerve ring

Cragi-CCK1: Crassostrea gigas (Magallana gigas) cholecystokinin 1

DMEM: dulbecco’s modified eagle’s medium

DMSO: dimethyl sulfoxide

DSK-R1: Drosophila melanogaster sulfakinin receptor 1

EC_{50}: half-maximal effective concentration

ERK1/2: extracellular signal regulated kinase 1/2

FBS: fetal bovine serum

FIR: feed intake rate

G5A: GFP-aequorin fusion protein

GLP-1: glucagon-like peptide-1

GPCR: G protein-coupled receptor

GRAVY: grand average of hydropathy

Kiss: kisspeptin

Luc: luciferase

MFP: ModelFinder Plus

ORF: open reading frame

PBS: phosphate buffer saline

p-ERK1/2: phosphorylated extracellular signal regulated kinase 1/2

PKA: protein kinase A

PKC: protein kinase C

pLDDT: per-residue confidence scores

RT-qPCR: reverse transcription-quantitative real-time polymerase chain reaction

SGR: specific growth rate

SK/CCK: sulfakinin/cholecystokinin

SK/CCKR: sulfakinin/cholecystokinin receptor

SRE/CRE: serum-responsive element/cAMP response element

t-ERK1/2: total extracellular signal regulated kinase 1/2

VP/OT: vasopressin/oxytocin

WGR: weight gain rate

Declarations

Ethics approval and consent to participate

All methods were carried out in accordance with the ARRIVE guidelines (https://arriveguidelines.org) for animal experiments. All animal care and use procedures were approved by the Institutional Animal Care and Use Committee of Ocean University of China (Permit Number: 20141201). They were performed according to the Chinese Guidelines for the Care and Use of Laboratory Animals (GB/T 35892–2018).

Consent for publication

Not applicable.

Data Availability and and materials

All datasets generated or analysed during this study are included in this published article and its supplementary additional files.

Competing interests

The authors declare that they have no competing interests.

Funding

This work was supported by National Natural Science Foundation of China [grant number 42276103].

Authors' contributions

M.C. planned and designed the project. H. L. H.Y. and X.T. performed the experimental work and/or analyzed experimental data. H. L. wrote the article and prepared the figures. M.C. and M.R.E. reviewed the manuscript and supervised the project. All authors read and approved the final version of the manuscript.

Acknowledgements

We thank Yingqiu Zheng for insightful comments during the manuscript preparation, and Xiaohan Zhang and Jianxuan Du for their assistance with the functional experiments and maintaining the aquaria. And we thank all the reviewers and academic editors for their work on this manuscript.

References

1. Chaudhri OB, Salem V, Murphy KG, Bloom SR. Gastrointestinal satiety signals. Annu Rev Physiol. 2008; 70, 239–255.

2. Andermann ML, Lowell BB. Toward a Wiring Diagram Understanding of Appetite Control. Neuron. 2017; 95(4), 757–778.

3. Thoma V, Sakai S, Nagata K, Ishii Y, Maruyama S, Abe A, et al. On the origin of appetite: GLWamide in jellyfish represents an ancestral satiety neuropeptide. Proc Natl Acad Sci U S A. 2023; 120(15), e2221493120.

4. Zhang G, Ding XY, Romanova EV, Liu CP, Barry MA, Doda A, et al. Synaptic and intrinsic plasticity mediated by CCK-type signaling coordinates behavioral changes during motivational state shifts. Cell Rep. 2025; 44(8), 116049.

5. Dockray GJ. Gastrointestinal hormones and the dialogue between gut and brain. J Physiol. 2014; 592(14), 2927–2941.

6. Woods SC, May-Zhang AA, Begg DP. How and why do gastrointestinal peptides influence food intake? Physiol Behav. 2018; 193(Pt B), 218–222.

7. Cawthon CR, de La Serre CB. The critical role of CCK in the regulation of food intake and diet-induced obesity. Peptides. 2021; 138, 170492.

8. Nässel DR, Wu SF. Cholecystokinin/sulfakinin peptide signaling: conserved roles at the intersection between feeding, mating and aggression. Cell Mol Life Sci. 2022; 79(3), 188.

9. Chowdhury S, Kamatkar NG, Wang WX, Akerele CA, Huang J, Wu J, et al. Brainstem neuropeptidergic neurons link a neurohumoral axis to satiation. Cell. 2025; 188(6), 1563–1579.

10. Santoso P, Nakata M, Ueta Y, Yada T. Suprachiasmatic vasopressin to paraventricular oxytocin neurocircuit in the hypothalamus relays light reception to inhibit feeding behavior. Am J Physiol Endocrinol Metab. 2018; 315(4), E478–E488.

11. Wang T, Cao Z, Shen Z, Yang J, Chen X, Yang Z, et al. Existence and functions of a kisspeptin neuropeptide signaling system in a non-chordate deuterostome species. ELife. 2020; 9, e53370.

12. Guo D, Zhang YJ, Zhang S, Li J, Guo C, Pan YF, et al. Cholecystokinin-like peptide mediates satiety by inhibiting sugar attraction. PLoS Genet. 2021; 17(8), e1009724.

13. Tinoco AB, Barreiro-Iglesias A, Yañez Guerra LA, Delroisse J, Zhang Y, Gunner EF, et al. Ancient role of sulfakinin/cholecystokinin-type signalling in inhibitory regulation of feeding processes revealed in an echinoderm. ELife. 2021; 10, e65667.

14. Roth E, Benoit S, Quentin B, Lam B, Will S, Ma M, et al. Behavioural and neurochemical

mechanisms underpinning the feeding-suppressive effect of GLP-1/CCK combinatorial therapy. Mol Metab. 2021; 43, 101118.

15. Hudson AD, Kauffman AS. Metabolic actions of kisspeptin signaling: Effects on body weight, energy expenditure, and feeding. Pharmacol Ther. 2022; 231, 107974.

16. Cong X, Liu H, Zheng Y, Chen M. A Putative Role of Vasopressin/Oxytocin-Type Neuropeptide in Osmoregulation and Feeding Inhibition of *Apostichopus japonicus*. Int J Mol Sci. 2023; 24(18), 14358.

17. Ivy AC, Oldberg E. A hormone mechanism for gall-bladder contraction and evacuation. American Journal of Physiology-Legacy Content. 1928; 86(3), 599-613.

18. Koopmans HS, Deutsch JA, Branson PJ. The effect of cholecystokinin pancreozymin on hunger and thirst in mice. Behav Biol. 1972; 7(3), 441–444.

19. Chandra R, Liddle RA. Cholecystokinin. Curr Opin Endocrinol Diabetes Obes. 2007; 14(1), 63–67.

20. Asim M, Wang H, Waris A, Qianqian G, Chen X. Cholecystokinin neurotransmission in the central nervous system: Insights into its role in health and disease. Biofactors. 2024; 50(6):1060-1075.

21. Gregory H, Hardy PM, Jones DS, Kenner GW, Sheppard RC. The antral hormone gastrin. structure of gastrin. Nature. 1964; 204, 931–933.

22. Mutt V, Jorpes JE. Structure of Porcine Cholecystokinin-Pancreozymin: 1. Cleavage with Thrombin and with Trypsin. Eur J Biochem. 1968; 6(1), 156-162.

23. Monstein HJ, Thorup JU, Folkesson R, Johnsen AH, Rehfeld JF. cDNA deduced procionin. Structure and expression in protochordates resemble that of procholecystokinin in mammals. FEBS Lett. 1993; 331(1-2), 60–64.

24. Dupré D, Tostivint H. Evolution of the gastrin-cholecystokinin gene family revealed by synteny analysis. Gen Comp Endocrinol. 2014; 195, 164–173.

25. Nachman RJ, Holman GM, Haddon WF, Ling N. Leucosulfakinin, a sulfated insect neuropeptide with homology to gastrin and cholecystokinin. Science. 1986; 234(4772), 71–73.

26. Janssen T, Meelkop E, Lindemans M, Verstraelen K, Husson SJ, Temmerman L, et al. Discovery of a cholecystokinin-gastrin-like signaling system in nematodes. Endocrinology. 2008; 149(6), 2826–2839.

27. Gibbs S, DeGolier TF. Neurotensin and cholecystokinin depress motility in isolated Lumbricus terrestris crop-gizzard preparations. Comp Biochem Physiol A Mol Integr Physiol. 2008; 151(4), 682–686.

28. Schwartz J, Dubos MP, Pasquier J, Zatylny-Gaudin C, Favrel P. Emergence of a cholecystokinin/sulfakinin signalling system in Lophotrochozoa. Sci Rep. 2018; 8(1), 16424.

29. de Weerth A, Pisegna JR, Huppi K, Wank SA. Molecular cloning, functional expression and chromosomal localization of the human cholecystokinin type A receptor. Biochem Biophys Res Commun. 1993; 194(2), 811–818.

30. Dufresne M, Seva C, Fourmy D. Cholecystokinin and gastrin receptors. Physiol Rev. 2006; 86(3), 805–847.

31. Nichols R. The first nonsulfated sulfakinin activity reported suggests nsDSK acts in gut biology. Peptides. 2007; 28(4), 767–773.

32. Rehfeld JF. Cholecystokinin-from local gut hormone to ubiquitous messenger. Front Endocrinol (Lausanne). 2017; 8, 47.

33. Torsoli A, Ramorino ML, Colagrande C, Demaio G. Experiments with cholecystokinin. Acta Radiol (Stockh). 1961; 55, 193–206.

34. Behar J, Biancani P. Effect of cholecystokinin-octapeptide on lower esophageal sphincter. Gastroenterology. 1977; 73(1), 57–61.

35. Hauser F, Williamson M, Cazzamali G, Grimmelikhuijzen CJ. Identifying neuropeptide and protein hormone receptors in *Drosophila melanogaster* by exploiting genomic data. Brief Funct Genomic Proteomic. 2006; 4(4), 321–330.

36. Hauser F, Neupert S, Williamson M, Predel R, Tanaka Y, Grimmelikhuijzen CJ. Genomics and peptidomics of neuropeptides and protein hormones present in the parasitic wasp *Nasonia vitripennis*. J Proteome Res. 2010; 9(10), 5296–5310.

37. Yu N, Smagghe G. CCK(-like) and receptors: structure and phylogeny in a comparative perspective. Gen Comp Endocrinol. 2014; 209, 74–81.

38. Nachman RJ, Giard W, Favrel P, Suresh T, Sreekumar S, Holman GM. Insect myosuppressins and sulfakinins stimulate release of the digestive enzyme α-amylase in two invertebrates: the scallop *Pecten maximus* and insect *Rhynchophorus ferrugineus*. Ann N Y Acad Sci. 1997; 814(1), 335-338.

986 39. Pangestuti R, Arifin Z. Medicinal and health benefit effects of functional sea cucumbers. J
987 Tradit Complement Med. 2017; 8(3), 341–351.
988 40. Guo K, Su L, Wang Y, Liu H, Lin J, Cheng P, et al. Antioxidant and anti-aging effects of a
989 sea cucumber protein hydrolyzate and bioinformatic characterization of its composing peptides.
990 Food Funct. 2020; 11(6), 5004–5016.
991 41. Oh DY, Song JA, Moon JS, Moon MJ, Kim JI, Kim K, et al. Membrane-proximal region of
992 the carboxyl terminus of the gonadotropin-releasing hormone receptor (GnRHR) confers
993 differential signal transduction between mammalian and nonmammalian GnRHRs. Mol
994 Endocrinol. 2005; 19(3), 722–731.
995 42. Sutton GM, Patterson LM, Berthoud HR. Extracellular signal-regulated kinase 1/2 signaling
996 pathway in solitary nucleus mediates cholecystokinin-induced suppression of food intake in
997 rats. J Neurosci. 2004; 24(45), 10240–10247.
998 43. Ge J, Ye L, Cheng M, Xu W, Chen Z, Guan F. Preparation of microgels loaded with
999 lycopene/NMN and their protective mechanism against acute liver injury. Food Funct. 2024;
1000 15(2):809-822.
1001 44. Liu Q, Yang D, Zhuang Y, Croll TI, Cai X, Dai A, et al. Ligand recognition and G-protein
1002 coupling selectivity of cholecystokinin A receptor. Nat Chem Biol. 2021; 17(12), 1238–1244.
1003 45. Mobbs JI, Belousoff MJ, Harikumar KG, Piper SJ, Xu X, Furness SGB, et al. Structures of
1004 the human cholecystokinin 1 (CCK1) receptor bound to Gs and Gq mimetic proteins provide
1005 insight into mechanisms of G protein selectivity. PLoS Biol. 2021; 19(6), e3001295.
1006 46. Staljanssens D, Azari EK, Christiaens O, Beaufays J, Lins L, Van Camp J, et al. The CCK(-
1007 like) receptor in the animal kingdom: functions, evolution and structures. Peptides. 2011; 32(3),
1008 607–619.
1009 47. Zheng Y, Cong X, Liu H, Storey KB, Chen M. Neuronal cell populations in circumoral nerve
1010 ring of sea cucumber *Apostichopus japonicus*: Ultrastructure and transcriptional profile. Comp
1011 Biochem Physiol Part D Genomics Proteomics. 2024; 52, 101263.
1012 48. Deribe Y L, Wild P, Chandrashaker A, Curak J, Schmidt MHH, Kalaidzidis Y, et al.
1013 Regulation of epidermal growth factor receptor trafficking by lysine deacetylase HDAC6. Sci
1014 Signal. 2009; 2(102): ra84-ra84.
1015 49. Li S, Zhou Z, Dong Y, Sun H, Gao S, Chen Z, et al. Molecular characterization, expression

1016 analysis of the myostatin gene and its association with growth traits in sea cucumber
1017 (*Apostichopus japonicus*). Comp Biochem Physiol B Biochem Mol Biol. 2016; 201, 12–20.
1018 50. Cong X, Liu H, Liu L, Escudero Castelán N, Jones KGE, Egertová M, et al. Functional
1019 characterization of neuropeptides that act as ligands for both calcitonin-type and pigment-
1020 dispersing factor-type receptors in a deuterostome. Elife. 2025; 13:RP101799.
1021 51. McPherron AC, Lawler AM, Lee SJ. Regulation of skeletal muscle mass in mice by a new
1022 TGF-beta superfamily member. Nature. 1997; 387(6628), 83–90.
1023 52. Semmens DC, Mirabeau O, Moghul I, Pancholi MR, Wurm Y, Elphick MR. Transcriptomic
1024 identification of starfish neuropeptide precursors yields new insights into neuropeptide evolution.
1025 Open Biol. 2016; 6(2):150224.
1026 53. Zandawala M, Moghul I, Yañez Guerra LA, Delroisse J, Abylkassimova N, Hugall AF, et al.
1027 Discovery of novel representatives of bilaterian neuropeptide families and reconstruction of
1028 neuropeptide precursor evolution in ophiuroid echinoderms. Open Biol. 2017; 7(9), 170129.
1029 54. Chen M, Talarovicova A, Zheng Y, Storey KB, Elphick MR. Neuropeptide precursors and
1030 neuropeptides in the sea cucumber *Apostichopus japonicus*: a genomic, transcriptomic and
1031 proteomic analysis. Sci Rep. 2019; 9(1), 8829.
1032 55. Aleotti A, Wilkie IC, Yañez-Guerra LA, Gattoni G, Rahman TA, Wademan RF, et al.
1033 Discovery and functional characterization of neuropeptides in crinoid echinoderms. Front
1034 Neurosci. 2022; 16, 1006594.
1035 56. Johnsen AH, Duve H, Davey M, Hall M, Thorpe A. Sulfakinin neuropeptides in a crustacean.
1036 Isolation, identification andtissue localization in the tiger prawn *Penaeus monodon*. Eur J
1037 Biochem. 2000; 267(4), 1153–1160.
1038 57. Derst C, Dircksen H, Meusemann K, Zhou X, Liu S, Predel R. Evolution of neuropeptides
1039 in non-pterygote hexapods. BMC Evol Biol. 2016; 16, 51.
1040 58. Yeoh JGC, Pandit AA, Zandawala M, Nässel DR, Davies SA, Dow JAT. DINeR: Database
1041 for Insect Neuropeptide Research. Insect Biochem Mol Biol. 2017; 86, 9–19.
1042 59. Wan Y, Deng Q, Zhou Z, Deng Y, Zhang J, Li J, et al. Cholecystokinin (CCK) and its
1043 receptors (CCK1R and CCK2R) in chickens: functional analysis and tissue expression. Poult
1044 Sci. 2023; 102(1), 102273.
1045 60. Kubiak TM, Larsen MJ, Burton KJ, Bannow CA, Martin RA, Zantello MR, et al. Cloning and

1046 functional expression of the first *Drosophila melanogaster* sulfakinin receptor DSK-R1.
1047 Biochem Biophys Res Commun. 2002; 291(2), 313–320.
1048 61. Zels S, Verlinden H, Dillen S, Vleugels R, Nachman RJ, Vanden Broeck J. Signaling
1049 properties and pharmacological analysis of two sulfakinin receptors from the red flour beetle,
1050 *Tribolium castaneum*. PLoS One. 2014; 9(4), e94502.
1051 62. Pace CN. Energetics of protein hydrogen bonds. Nat Struct Mol Biol. 2009; 16(7), 681–682.
1052 63. Pace CN, Fu H, Lee Fryar K. Landua J, Trevino SR, Schell D, et al. Contribution of hydrogen
1053 bonds to protein stability. Protein Sci. 2014; 23(5), 652–661.
1054 64. Tan KP, Singh K, Hazra A, Madhusudhan MS. Peptide bond planarity constrains hydrogen
1055 bond geometry and influences secondary structure conformations. Curr Res Struct Biol. 2020;
1056 3, 1–8.
1057 65. Tinoco AB, Kirupakaran V, Capatina D, Egertová M, Elphick MR. Discovery of a
1058 neuropeptide that acts as an autotomy-promoting factor. Curr Biol. 2024; 34(18):4325-4331.e3.
1059 66. Brown NP, Eddy SD. Echinoderm Aquaculture (Hoboken: Wiley Blackwell). 2015.
1060 67. García-Arrarás JE, Torres-Avillán I, Ortíz-Miranda S. Cells in the intestinal system of
1061 holothurians (Echinodermata) express cholecystokinin-like immunoreactivity. Gen Comp
1062 Endocrinol. 1991; 83(2):233-42.
1063 68. Le HTMD, Lie KK, Giroud-Argoud J, Rønnestad I, Sæle Ø. Effects of cholecystokinin (CCK)
1064 on gut motility in the stomachless fish ballan wrasse (*Labrus bergylta*). Front Neurosci. 2019;
1065 13, 553.
1066 69. Tinoco AB, Valenciano AI, Gómez-Boronat M, Blanco AM, Nisembaum LG, De Pedro N, et
1067 al. Two cholecystokinin receptor subtypes are identified in goldfish, being the CCKAR involved
1068 in the regulation of intestinal motility. Comp Biochem Physiol A Mol Integr Physiol. 2015; 187,
1069 193–201.
1070 70. Zheng Y, Liu H, Cong X, Storey KB, Chen M. A potential feeding regulation strategy during
1071 aestivation: Relaxation of intestine mediated by pedal peptide/orcokinin-type neuropeptides in
1072 sea cucumber *Apostichopus japonicus*. Aquaculture. 2024; 579, 740150.
1073 71. Olsson C, Aldman G, Larsson A, Holmgren S. Cholecystokinin affects gastric emptying and
1074 stomach motility in the rainbow trout *Oncorhynchus mykiss*. J Exp Biol. 1999; 202(Pt 2):161-
1075 70.

1076 72. Smith DM, Grasty RC, Theodosiou NA, Tabin CJ, Nascone-Yoder NM. Evolutionary
1077 relationships between the amphibian, avian, and mammalian stomachs. Evol Dev. 2000;
1078 2(6):348-59.
1079 73. Hunt RH, Camilleri M, Crowe SE, El-Omar EM, Fox JG, Kuipers EJ, et al. The stomach in
1080 health and disease. Gut. 2015; 64(10):1650-68.
1081 74. Kamenev YO, Dolmatov IY, Frolova LT, Khang NA. The morphology of the digestive tract
1082 and respiratory organs of the holothurian *Cladolabes schmeltzii* (Holothuroidea,
1083 Dendrochirotida). Tissue Cell. 2013; 45(2):126-39.
1084 75. Yamagishi T, Debas HT. Cholecystokinin inhibits gastric emptying by acting on both
1085 proximal stomach and pylorus. Am J Physiol. 1978; 234(4):E375-8.
1086 76. Shimizu M, Mikami I, Takahashi K. Histochemical detection on the ontogenic development
1087 of digestive enzymes in the intestine of a juvenile sea cucumber *Stichopus japonicus*. Bulletin
1088 of the Faculty of Fisheries-Hokkaido University (Japan). 1994; 45(1).
1089 77. Pan W, Wang X, Ren C, Jiang X, Gong S, Xie Z, et al. Sea cucumbers and their symbiotic
1090 microbiome have evolved to feed on seabed sediments. Nat Commun. 2024; 15(1):8825.
1091 78. Antin J, Gibbs J, Holt J, Young RC, Smith GP. Cholecystokinin elicits the complete
1092 behavioral sequence of satiety in rats. J Comp Physiol Psychol. 1975; 89(7):784-90.
1093 79. Miura T, Maruyama K, Shimakura S, Kaiya H, Uchiyama M, Kangawa K, et al. Regulation
1094 of food intake in the goldfish by interaction between ghrelin and orexin. Peptides. 2007; 28(6),
1095 1207–1213.
1096 80. Blais A, Drouin G, Chaumontet C, Voisin T, Couvelard A, Even PC, et al. Impact of Orexin-
1097 A Treatment on Food Intake, Energy Metabolism and Body Weight in Mice. PLoS One. 2017;
1098 12(1), e0169908.
1099 81. Soya S, Sakurai T. Evolution of orexin neuropeptide system: structure and function. Front
1100 Neurosci. 2020; 14, 691.
1101 82. Gallmann E, Arsenijevic D, Spengler M, Williams G, Langhans W. Effect of CCK-8 on
1102 insulin-induced hyperphagia and hypothalamic orexigenic neuropeptide expression in the rat.
1103 Peptides. 2005; 26(3), 437–445.
1104 83. Williams DL, Coiduras II, Parise EM, Maske CB. Hindbrain orexin 1 receptors blunt intake
1105 suppression by gastrointestinal nutrients and cholecystokinin in male rats. Peptides. 2020; 133,

170351.

84. Katoh K, Standley DM. MAFFT multiple sequence alignment software version 7: improvements in performance and usability. Mol Biol Evol. 2013; 30(4), 772–780.

85. Capella-Gutiérrez S, Silla-Martínez JM, Gabaldón T. trimAl: a tool for automated alignment trimming in large-scale phylogenetic analyses. Bioinformatics. 2009; 25(15), 1972–1973.

86. Nguyen LT, Schmidt HA, von Haeseler A, Minh BQ. IQ-TREE: a fast and effective stochastic algorithm for estimating maximum-likelihood phylogenies. Mol Biol Evol. 2015; 32(1), 268–274.

87. Kalyaanamoorthy S, Minh BQ, Wong TKF, von Haeseler A, Jermiin LS. ModelFinder: fast model selection for accurate phylogenetic estimates. Nat Methods. 2017; 14(6), 587–589.

88. Abramson J, Adler J, Dunger J, Evans R, Green T, Pritzel A, et al. Accurate structure prediction of biomolecular interactions with AlphaFold 3. Nature. 2024; 630(8016), 493–500.

89. Morris GM, Huey R, Lindstrom W, Sanner MF, Belew RK, Goodsell DS, et al. AutoDock4 and AutoDockTools4: Automated docking with selective receptor flexibility. J Comput Chem. 2009; 30(16), 2785–2791.

90. Eberhardt J, Santos-Martins D, Tillack AF, Forli S. AutoDock Vina 1.2.0: New Docking Methods, Expanded Force Field, and Python Bindings. J Chem Inf Model. 2021; 61(8), 3891–3898.

91. Laskowski RA, Swindells MB. LigPlot+: multiple ligand-protein interaction diagrams for drug discovery. J Chem Inf Model. 2011; 51(10), 2778–2786.

92. Zhao Y, Chen M, Wang T, Sun L, Xu D, Yang H. Selection of reference genes for RT-qPCR analysis of gene expression in sea cucumber *Apostichopus japonicus* during aestivation. Chin J Oceanol Limnol. 2014; 32(6), 1248-1256.

93. Liu Y, He G, Wang Q, Mai K, Xu W, Zhou H. Hydroxyproline supplementation on the performances of high plant protein source based diets in turbot (*Scophthalmus maximus L.*). Aquaculture. 2014; 433, 476-480.

94. Wang Z, Cui J, Song J, Wang H, Gao K, Qiu X, et al. Comparative Transcriptome Analysis Reveals Growth-Related Genes in Juvenile Chinese Sea Cucumber, Russian Sea Cucumber, and Their Hybrids. Mar Biotechnol. 2018; 20(2), 193–205.

Supplementary data

Additional file 1:

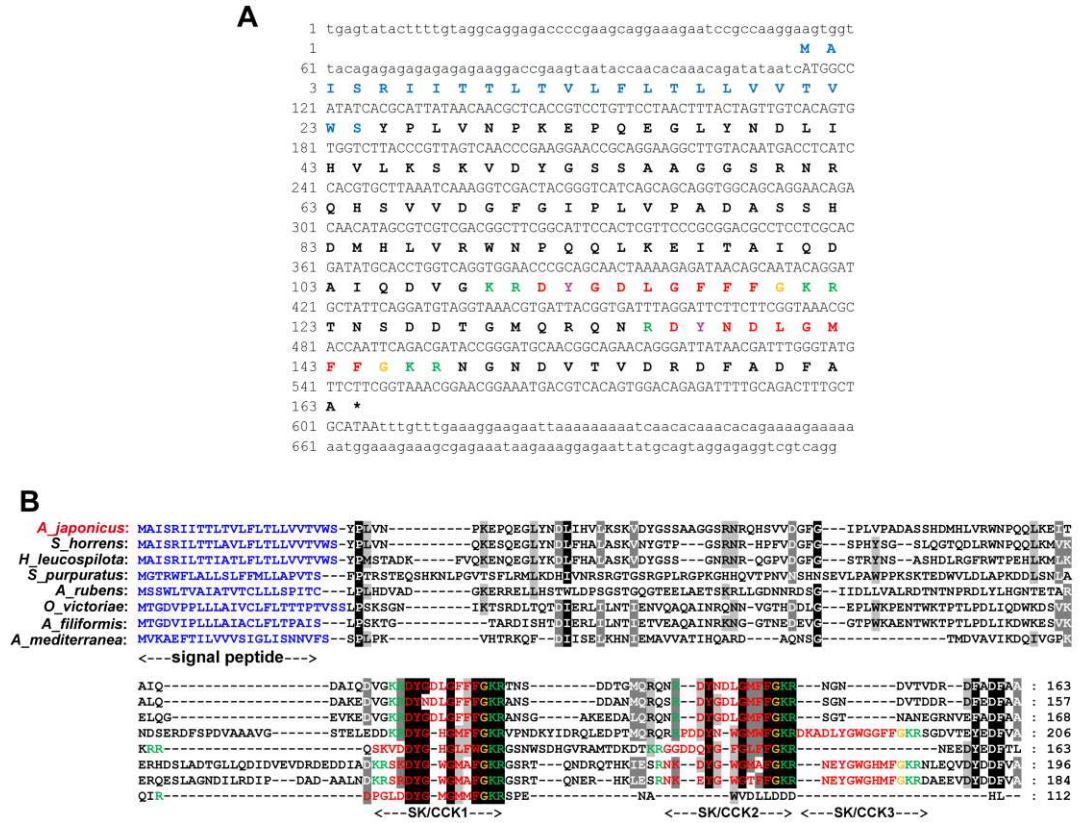

Fig. S1. Molecular characterization of SK/CCK-type neuropeptide precursors in echinoderms

A: Nucleotide sequence of AjSK/CCK precursor (GenBank accession number: MH636358) and the deduced amino acid sequence. ORF is showed in uppercase; 3'UTR and 5'UTR is shown in lowercase. The predicted signal peptide is highlighted in blue, potential proteolytic cleavage sites in green, and SK/CCK-type peptides in red. C-terminal glycine (G) residues, putative substrates for amidation, are shown in orange and tyrosine (Y) residues predicted to be sulphated are in purple. B: Alignment of AjSK/CCKP with SK/CCK-type precursor proteins of other echinoderms, with the predicted signal peptides shown in blue, the potential proteolytic cleavage sites shown in green, predicted SK/CCK-type peptides shown in red and the C-terminal glycine residues which are the putative substrate for amidation shown in orange. Conserved residues are highlighted in black or gray, with 60 % conservation as a minimum for highlighting.

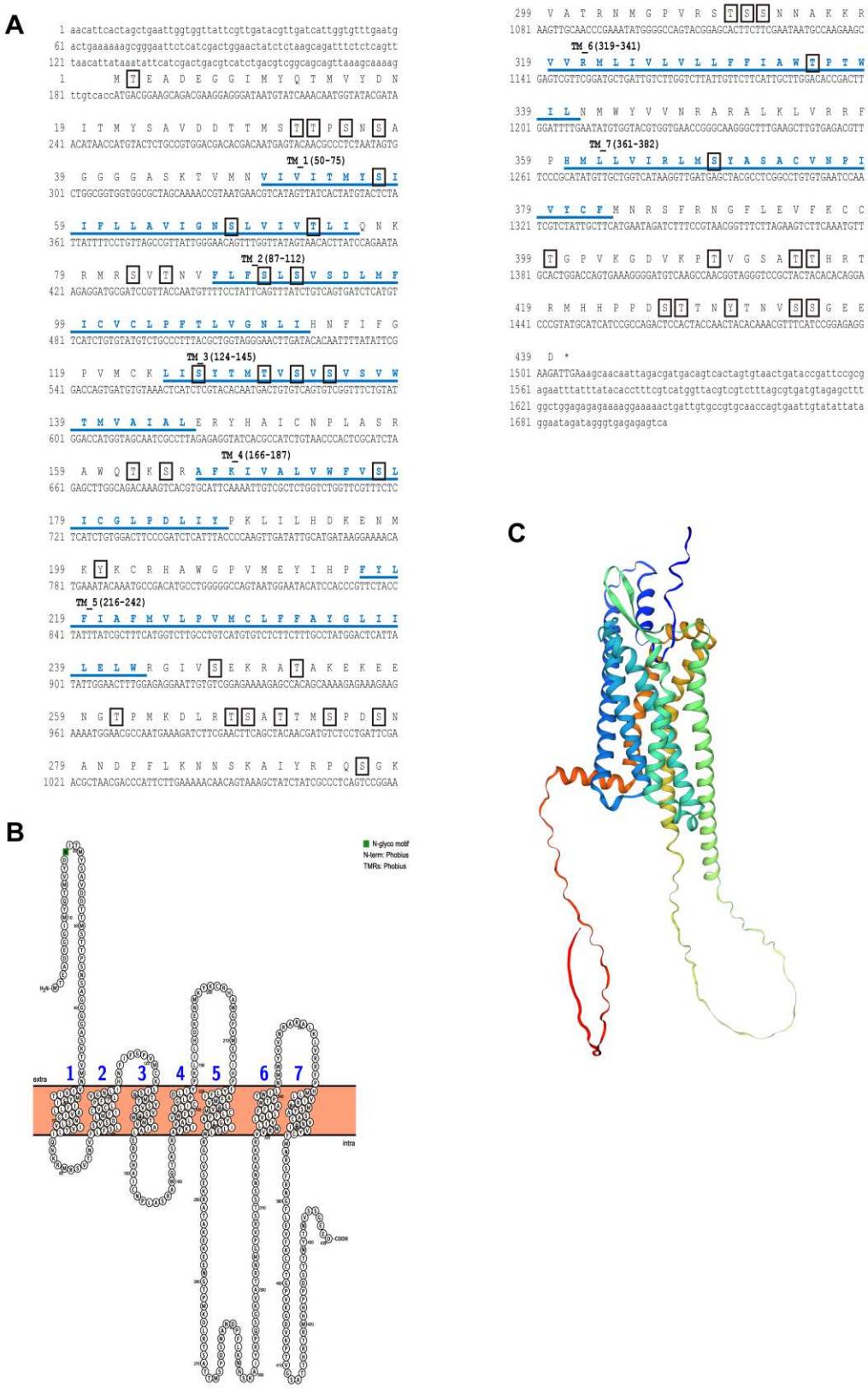

Fig. S2. Molecular structure and characterization of AjSK/CCKR in *A. japonicus*

A: AjSK/CCKR cDNA sequence and the deduced amino acid sequence. ORF is denoted in uppercase; 3'UTR and 5'UTR is shown in lowercase. The asterisk (*) indicates the stop codon.

The squares indicate potential phosphorylation sites. The seven transmembrane domains (TM1-TM7) are labeled in blue. B: Predicted topology of AjSK/CCKR. The numbers in blue show the positions of the seven transmembrane domains and the residue shown in green is a potential site for glycosylation. C: Predicted tertiary structure of AjSK/CCKR as visualised using SWISS-MODEL.

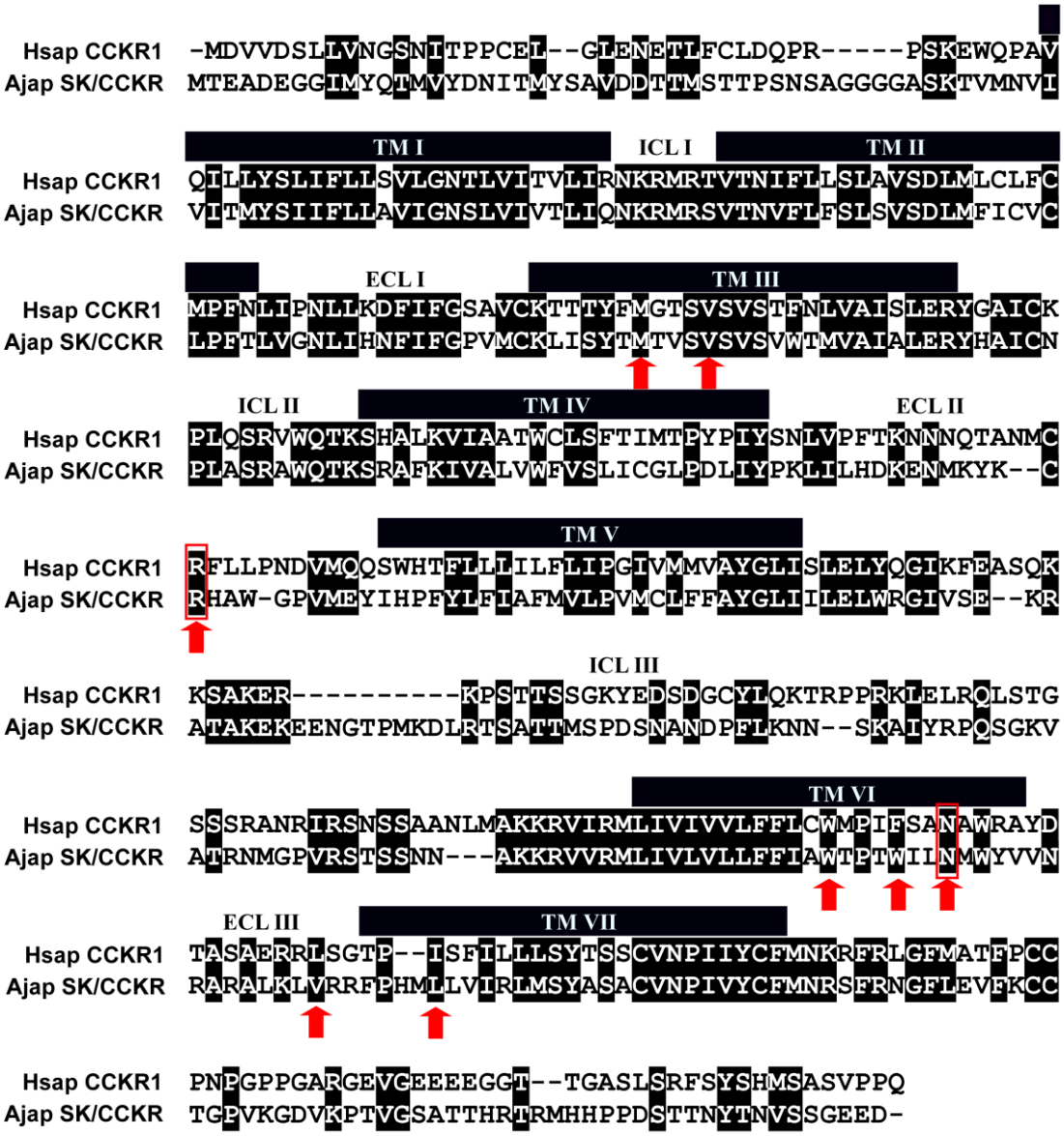

Fig. S3. Sequence alignment of AjSK/CCKR with human CCKR1

The seven transmembrane domains (TM I–VII) of human CCKR1 are delineated, along with its intracellular and extracellular loops. Conserved and similar residues are highlighted in black boxes. Conserved residues known or predicted to be involved in ligand binding in the two receptors are marked with red arrows. Arg203/Arg197 and Asn341/Asn333, which are known

or predicted to participate in hydrogen bonding with the ligands in *A. japonicus* and human, respectively, are highlighted with red boxes.

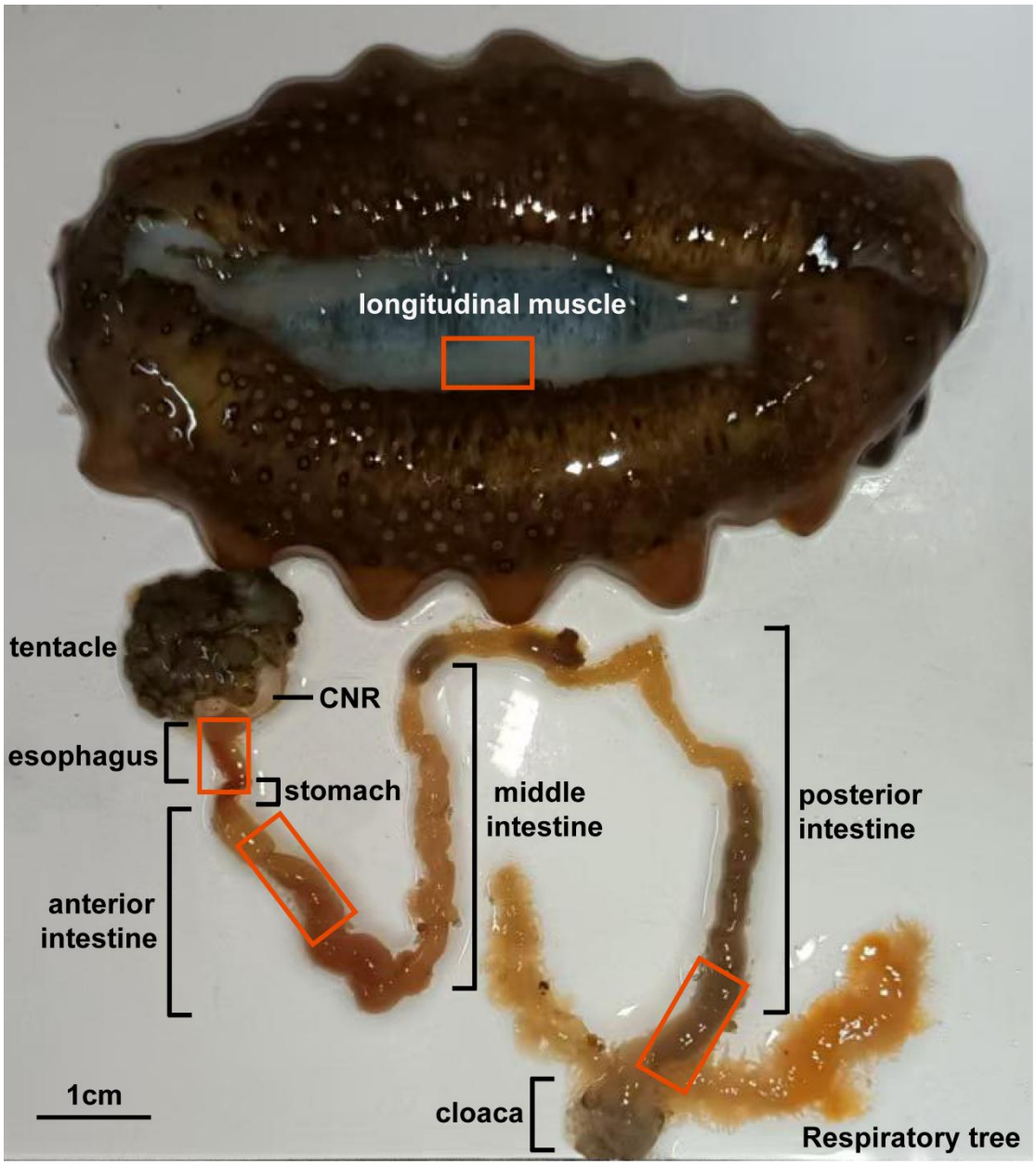

Fig. S4. Diagram of the *A. japonicus* digestive tract

The esophagus, stomach, anterior, middle, posterior intestine, and cloaca are shown. Regions marked with a red box (esophagus, anterior and posterior intestine, and longitudinal muscle) were selected for *in vitro* pharmacological assays. The middle intestine was excluded due to its lack of contractile responsiveness to acetylcholine.

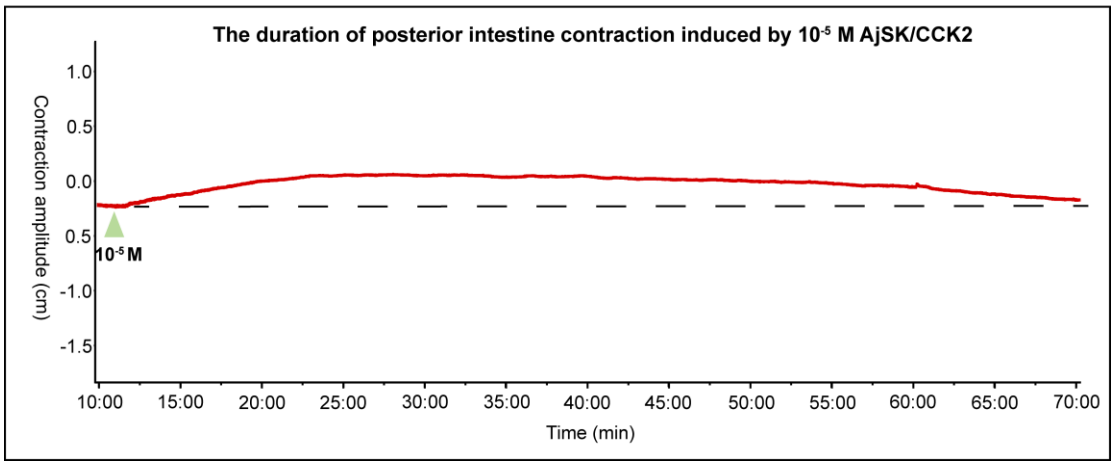

Fig. S5. The duration of posterior intestine contraction induced by 10^{-5} M AjSK/CCK2

The contraction duration was defined as the time interval from the initiation of contraction to the complete return to the pre-contraction baseline level.

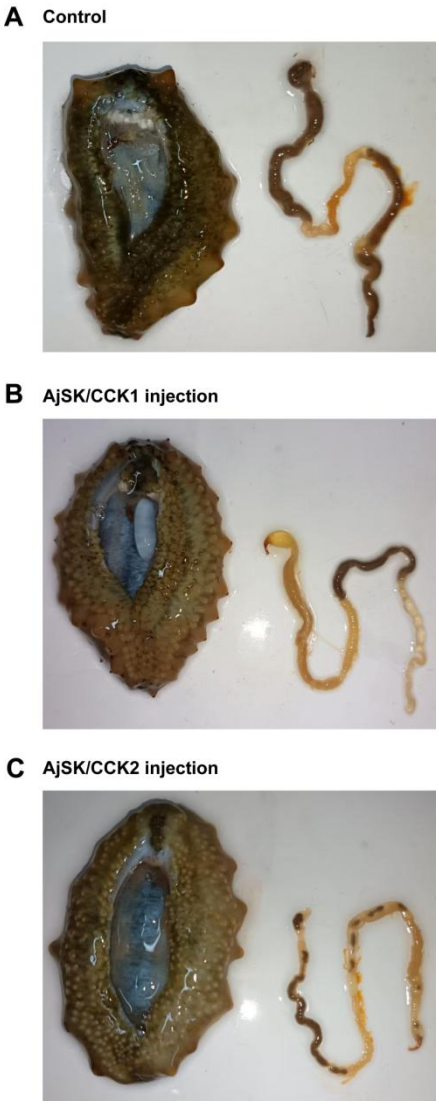

Fig. S6. Intestinal morphology of *A. japonicus* following chronic peptide administration

A: Intestine from the control group injected with PBS containing 1% DMSO. B: Intestine from the group injected with AjSK/CCK1. C: Intestine from the group injected with AjSK/CCK2.

Additional file 2: Dataset S1. Accession numbers for SK/CCK-type precursor sequences across bilaterian animals shown in the sequence alignment and the clustering analysis in **Fig. 1**.

Phylum	Species	Abbreviation	Accession number
Vertebrata	*Homo sapiens*	H_sap CCKP	AAA53094.1
	Homo sapiens	H_sap GastrinP	P01350
	Gallus gallus	G_gal CCKP	NP_001001741.1
	Emys orbicularis	E_orb CCKP	XP_065256082.1
	Xenopus laevis	X_lae CCKAP	NP_001079303.1
	Xenopus laevis	X_lae CCKBP	NP_001079304.1
	Carassius auratus	C_aur CCKP	XP_026139952.1
	Danio rerio	D_rer CCKP	XP_002665661.2
Urochordata	*Ciona intestinalis*	C_int CioninP	P16240
Hemichordate	*Saccoglossus kowalevskii*	S_kow SK/CCKP	XM_002738068.2
Echinodermata	*Apostichopus japonicus*	A_jap SK/CCKP	MH636358
	Stichopus horrens	S_hor SK/CCKP	HAMZ01045944.1
	Holothuria leucospilota	H_leu SK/CCKP	KAJ8019420.1
	Strongylocentrotus purpuratus	S_pur SK/CCKP	[11]
	Asterias rubens	A_rub SK/CCKP	ALJ99958.1
	Ophionotus victoriae	O_vic SK/CCKP	ASK86241.1
	Antedon mediterranea	A_med SK/CCKP	[44]
Annelida	*Urechis unicinctus*	U_uni SKP	QUP52013.1
	Capitella teleta	C_tel SKP	ELT92762.1
	Ridgeia piscesae	R_pis SKP	KAK2156806.1
	Paralvinella palmiformis	P_pal SKP	KAK2141978.1

Mollusca	*Aplysia californica*	A_cal CCKP	XP_005096263.1
	Crassostrea gigas	C_gig CCKP	[25]
	Crassostrea virginica	C_vir CCKP	XP_022326792.1
	Lymnaea stagnalis	L_sta CCKP	CAL1547016.1
	Bradybaena similaris	B_sim CCKP	BFZ21690.1
	Ambigolimax valentianus	A_val CCKP	BBD49873.1
	Deroceras reticulatum	D_ret CCKP	ARS01390.1
	Biomphalaria glabrata	B_gla CCKP	KAI8761131.1
Arthropoda	*Tribolium castaneum*	T_cas SKP	EFA04708.1
	Drosophila melanogaster	D_mel SKP	P09040
	Periplaneta americana	P_ame SKP	ALG35946.1
	Drosophila erecta	D_ere SKP	XP_001978781.1
	Neocloeon triangulifer	N_tri SKP	XP_059482729.1
	Myrmeleon formicarius	M_for SKP	CAN8925943.1
	Nilaparvata lugens	N_lug SKP	XP_039279256.1
	Bombyx mori	B_mor SKP	BAG49564.1
	Laodelphax striatellus	L_str SKP	RZF41044.1
	Lycorma delicatula	L_del SKP	XP_075214130.1
Nematoda	*Caenorhabditis elegans*	C_ele NP12	O01970
	Caenorhabditis auriculariae	C_aur NP12	CAD6186289.1
	Caenorhabditis bovis	C_bov NP12	CAB3407951.1
	Cylicocyclus nassatus	C_nas NP12	CAJ0592938.1

Additional file 3: Dataset S2. Accession numbers of the SK/CCK receptor sequences across bilaterian animals used for the phylogenetic analysis shown in **Fig. 2**.

Phylum	Species	Abbreviation	Accession number
Vertebrata	*Homo sapiens*	H_sap CCKR1	NP_000721.1
	Homo sapiens	H_sap CCKR2	NP_795344.1
	Mus musculus	M_mus CCKR1	NP_033957.1

	Mus musculus	M_mus CCKR2	NP_031653.1
	Gallus gallus	G_gal CCKR1	BAJ46148.1
	Gallus gallus	G_gal CCKR2	NP_001001742.1
	Emys orbicularis	E_orb CCKR	XP_065261570.1
	Xenopus laevis	X_lae CCKR	NP_001079277.1
	Danio rerio	D_rer CCKR1	XP_697493.2
	Danio rerio	D_rer CCKR2	XP_017213239.1
Urochordata	*Ciona intestinalis*	C_int CioR1	Q70SX9
	Ciona intestinalis	C_int CioR2	XP_018670223.1
Hemichordata	*Saccoglossus kowalevskii*	S_kow SK/CCKR1	XP_006814715.1
	Saccoglossus kowalevskii	S_kow SK/CCKR2	XP_006814705.1
Echinodermata	*Ophionotus victoriae*	O_vic SK/CCKR	MW261741.1
	Asterias rubens	A_rub SK/CCKR	MW261740
	Strongylocentrotus purpuratus	S_pur SK/CCKR	XP_782630.3
	Apostichopus japonicus	A_jap SK/CCKR	XP_071847465.1
	Holothuria leucospilota	H_leu SK/CCKR	KAJ8028236.1
	Lytechinus variegatus	L_var SK/CCKR	XP_041457523.1
	Acanthaster planci	A_pla SK/CCKR	XP_022079611.1
	Amphiura filiformis	A_fil SK/CCKR	XP_072040880.1
Annelida	*Capitella teleta*	C_tel CCKR	ELT89517.1
	Glossoscolex paulistus	G_pau CCKR	GBIL01035016.1
Mollusca	*Aplysia californica*	A_cal CCKR1	XP_012941704.2
	Magallana gigas	M_gig CCKR1	MF787221
	Magallana gigas	M_gig CCKR2	MF787222
	Crassostrea virginica	C_vir CCKR1	XP_022323244.1
	Crassostrea virginica	C_vir CCKR2	XP_022320712.1
	Lottia gigantea	L_gig CCKR1	XP_009047144.1
	Lottia gigantea	L_gig CCKR2	XP_009047126.1

	Ostrea edulis	O_edu CCKR1	XP_048756705.2
	Ostrea edulis	O_edu CCKR2	XP_048778710.1
Arthropoda	*Drosophila melanogaster*	D_mel SKR1	NP_001097023.1
	Drosophila melanogaster	D_mel SKR2	NP_001097021.1
	Tribolium castaneum	T_cas SKR1	XP_015835017.1
	Tribolium castaneum	T_cas SKR2	XP_972750.1
	Rhodnius prolixus	R_pro SKR1	MK513659
	Rhodnius prolixus	R_pro SKR2	MK513660
	Zophobas morio	Z_mor SKR1	XP_063923366.1
	Zophobas morio	Z_mor SKR2	XP_063903995.1
	Tenebrio molitor	T_mol SKR1	KAJ3631073.1
	Tenebrio molitor	T_mol SKR2	XP_068907312.1
Nematoda	*Caenorhabditis briggsae*	C_bri CKR1	XP 002640196.1
	Caenorhabditis briggsae	C_bri CKR2	XP 002642853.1
	Caenorhabditis elegans	C_ele CKR1	NP 491918.2
	Caenorhabditis elegans	C_ele CKR2a	ACA81683.1
	Caenorhabditis elegans	C_ele CKR2b	ACA81684.1
	Caenorhabditis remanei	C_rem CKR1	XP_003114892.1
	Caenorhabditis remanei	C_rem CKR2	XP_003103966.1
Out group	*Acanthaster planci* OrexinR1		XP_022107462.1
	Acanthaster planci OrexinR2		XP_022089610.1
	Strongylocentrotus purpuratus OrexinR1		XP_030838918.1
	Strongylocentrotus purpuratus OrexinR2		XP_030833857.1
	Apostichopus japonicus OrexinR1		XP_071836991.1

	Apostichopus japonicus OrexinR2		XP_071842539.1
	Saccoglossus kowalevskii OrexinR1		NP_001161621.1
	Saccoglossus kowalevskii OrexinR2		XP_002733613.1
	Homo sapiens OrexinR1		NP_001516.2
	Homo sapiens OrexinR2		NP_001517.2
	Gallus gallus OrexinR2		BAD72879.1
	Anolis carolinensis OrexinR2		XP_003226120.2
	Trachemys scripta elegans OrexinR2		XP_034622910.1
	Xenopus laevis OrexR2		XP_018118957.1
	Danio rerio OrexinR2		ABO61386.1
	Branchiostoma belcheri OrexinR1		XP_019619548.1
	Branchiostoma belcheri OrexinR2		XP_019619556.1

Additional file 4: Dataset S3. Primers used for High Fidelity PCR, RT-qPCR analysis and Plasmid construction.

AjCCKP-F	ATGGCCATATCACGCATTAT	High Fidelity PCR
AjCCKP-R	TTATGCAGCAAAGTCTGCAA	
AjCCKR-F	ACCATGACGGAAGCAGACGAAG	
AjCCKR-R	TCAATCTTCCTCTCCGGATGAAACG	
AjCCKR-pcDNA3.1(+)-F	TAAACTTAAGCTTGGTACCGAGCTCGGATCCACC ATGACGGAAGCAGACGAAG	pcDNA3.1(+) plasmid

AjCCKR-pcDNA3.1(+)-R	GCCGCCACTGTGCTGGATATCTGCAGAATTCTCA ATCTTCCTCTCCGGATGAAACG	constructed
AjGDF-8-F	CTTTCACCGTAAGGAGGAG	RT-qPCR
AjGDF-8-R	TCGGCATAGGATTTAGAGTA	
AjMegf6-F	CGGTCCTTACTGTGCGGAGA	
AjMegf6-R	CGTCCTCCCAGCTGGACATC	
Ajlgf-F	TGGAAGGCAGTAAGGCTA	
Ajlgf-R	TAGGCTGATGTGGTTGGA	
AjOrexinP1-F	CCTCCTCCTCCTCAACAT	
AjOrexinP1-R	GTGCTCGTCGTGATAGTC	
AjOrexinP2-F	TTGTTCCAAGATCCGTGATT	
AjOrexinP2-R	TTCCAGCGTATGTCCGAT	
β-Actin-F	AAGGTTATGCTCTTCCTCACGCT	
β-Actin-R	GATGTCACGGACGATTTCACG	
β-Tubulin-F	GAAAGCCTTACGACGGAACA	
β-Tubulin-R	CACCACGTGGACTCAAAATG	